EXPERIMENTAL INVESTIGATION OF SYNGAS FLAME STABILITY USING A MULTI-TUBE FUEL INJECTOR IN A HIGH PRESSURE COMBUSTOR

SERGIO ELZAR MALDONADO JURADO

Department of Mechanical Engineering

APPROVED:

Norman D. Love , Ph.D., Chair

Ahsan Choudhuri, Ph.D.

Heidi Taboada-Jimenez, Ph.D.

Charles H. Ambler, Ph.D.
Dean of the Graduate School

Copyright ©

by

Sergio E. Maldonado

2014

Dedication

To my family that has always supported me, my friends and roommates that have become my family, and the love of my life that has always motivated me to be a better person.

EXPERIMENTAL INVESTIGATION OF SYNGAS FLAME STABILITY USING A MULTI-TUBE FUEL INJECTOR IN A HIGH PRESSURE COMBUSTOR

by

SERGIO ELZAR MALDONADO, B.S.M.E.

THESIS

Presented to the Faculty of the Graduate School of

The University of Texas at El Paso

in Partial Fulfillment

of the Requirements

for the Degree of

MASTER OF SCIENCE

Department of Mechanical Engineering

THE UNIVERSITY OF TEXAS AT EL PASO

August 2014

UMI Number: 1564684

UMI

Dissertation Publishing

UMI 1564684

ProQuest

ProQuest LLC.
789 East Eisenhower Parkway
P.O. Box 1346
Ann Arbor, MI 48106 - 1346

www.manaraa.com

Acknowledgements

First, I would like to thank my parents and my family for allowing me to pursue my dream to study in the United States.

I would like to express my gratitude to all my friends that have always supported me and have become my family throughout this time. Thanks for guiding me, for motivating me during hard times and to inspire me to work hard to achieve what I want. I would like to thank Manny Pacillas for always supporting me, and inspiring me to believe in myself. To Ingrid Wright for all the many ways she had supported me throughout my career. To Rick O'Brien, leadership coach, but most importantly, my friend. Thank you to all the Baja SAE UTEP 2014 leadership team, for allowing me to be part of your lives in one of the most amazing experiences in my life.

I would like to give special thanks to my graduate advisor Dr. Norman Love, for allowing to me to work with him throughout my graduate studies. Thank you for teaching me something new every day and allowing me to love what I do. Thank you for your patience and for your support through hard times. Special thanks go to Dr. Ahsan R. Choudhuri for supporting me throughout my graduate studies and always motivating me to give the best of me. Thank you for challenging me in projects that shaped my personal and professional development. I would like to thank Dr. Heidi Taboada-Jimenez for her valuable input in my professional career.

I would like to thank Martin de La Torre, Jorge Rosero, Manny Hernandez, Sarzina Hossain, Sudipa Sarker, Carlos Valdez and Jesus Nunez for all their hard work in our High Pressure Combustion Group. This work is only possible because of their hard work and dedication.

Big thanks go to the Mechanical Engineering Staff Carmen Medellin, Laura Orozco, Ethel Martinez, Gloria Salas and Alejandra Garibaldi, for being my unconditional friends and supporting me throughout my entire career.

Finally, I would like to thank Marketka Vavrova, for being my support, my strength, and for giving me so much love. Thank you for inspiring me to work hard every day to achieve my dreams.

Abstract

Over 92% of the coal consumed by power plants is used to generate electricity in the United States (U.S.). The U.S. has the world's largest recoverable reserves of coal, it is estimated that reserves of coal will last more than 200 years based in current production and demand levels. Integrated Gasification Combined Cycle (IGCC) power plants aim to reduce the amount of pollutants by gasifying coal and producing synthesis gas. Synthesis gas, also known as syngas, is a product of coal gasification and can be used in gas turbines for energy production. Syngas is primarily a mixture of hydrogen and carbon monoxide and is produced by gasifying a solid fuel feedstock such as coal or biomass. The objective of the thesis is to create a flame stability map by performing various experiments using high-content hydrogen fuels with varying compositions of hydrogen representing different coal feedstocks. The experiments shown in this thesis were performed using the High-Pressure Combustion facility in the Center for Space Exploration Technology Research (CSETR) at the University of Texas at El Paso (UTEP). The combustor was fitted with a novel Multi-Tube fuel Injector (MTI) designed to improve flame stability. This thesis presents the results of testing of syngas fuels with compositions of 20, 30, and 40% hydrogen concentrations in mixtures with carbon monoxide. Tests were completed for lean conditions ranging from equivalence ratios between 0.6 and 0.9. The experimental results showed that at an equivalence ratio of 0.6, a stable flame was not achieved for any of the fuel mixtures tested. It was also observed that the stability region of the syngas flame increased as equivalence ratio and the hydrogen concentration in syngas fuel increases with the 40% hydrogen-carbon monoxide mixture demonstrating the greatest stability region. Design improvements to the MTI are also discussed as part of the future work on this topic.

Table of Contents

List of Tables

List of Figures

Chapter 1: Introduction

1.1   Introduction

Over 92% of the coal consumed by power plants is used to generate electricity in the United States. The U.S. has the world's largest recoverable reserves of coal, in fact, it is estimated that reserves of coal will last more than 200 years based in current production and demand levels. There are over 600 power plants and 1,400 coal-fired electricity generating units in the United States. According to the U.S. Energy Information Administration, 37% of the electricity generated in 2012 used coal. The United States has relied on coal for electricity generation over the past 60 years; however its use has declined from 50% in 2007 to 37% in 2012 due to the lower price of natural gas [1].

Gas and steam turbines are widely used for power generation in the United States. Gas turbines are internal combustion engines that consist of three main parts: Compressor, Combustor, and Turbine. The compressor section draws air into the engine, pressurizes it, and feeds it to the combustion chamber at high speeds. Compressed air enters the combustion chamber, it is premixed with fuel and ignited; the combustion produces a high temperature, high pressure gas stream that enter and expands to the turbine section. The hot gases from the combustor chamber expand through the turbine which causes the rotating blades to spin. The spinning shaft is subsequently connected to a generator to produce energy. [2]

Steam turbines are one of the most versatile and older prime mover technologies still in general production used to drive a power generator or any other mechanical machinery. Unlike gas turbines, steam turbines generate electricity as a byproduct of heat generation generally in form of steam. [3]
Coal fired power plants produce high amount of pollutants. Coal accounted for 31% of the energy-related carbon dioxide emission in the United States in 2012 [1]. In order to reduce the amount of

pollutant emitted by coal fired power plants, the Environmental Protection Agency (EPA) has released a series of regulations and restrictions in the use of coal of energy production.

Integrated Gasification Combined Cycle (IGCC) power plants aim to reduce the amount of pollutants by gasifying coal and producing synthesis gas, and by sequestrating CO_2 emissions from the gasification process. Synthesis gas, also known as syngas is a product of coal gasification and can be used in gas turbines for energy production. IGCC power plants produce energy with both steam and gas turbines. However the use of syngas introduces new challenges due to its high hydrogen content. New generation gas turbines must be able to operate with syngas.

1.2   Combustion

Combustion is defined as the rapid oxidation accompanied by light and heat. Combustion transforms the energy stored in the chemical bonds to heat and it can be utilized in a variety of ways. Combustion can occur in two modes: flame or non-flame. The flame modes can be categorized in non-premixed flames, also known as diffusion flames, and premixed flames [4].

Combustion can occur at 3 conditions: stoichiometric, lean, or rich. Stoichiometric combustion is the process in which the fuel is burned completely with the exact amount of oxidizer needed. On the other hand, when the fuel is burned completely but there is excess of oxidizer this is known as lean condition. Finally, when the fuel is not fully burned due to lack of oxidizer this is known as a rich combustion. The equivalence ratio (φ) is the parameter that helps to identify when combustion is categorized stoichiometric, lean, or rich. An equivalence ratio (φ) equal to 1 indicates a stoichiometric combustion, φ>1 indicates rich combustion and φ<1 indicates lean combustion.

1.3   Pollutant Emissions

Although coal is abundant and relatively cheap, its use produces several types of emissions that represent harm to the environment. According to the U.S. Energy Information Administration, coal accounted for 31% of the energy-related carbon dioxide emissions in the United States. Burning of solid coal also emits Sulfur Dioxide (SO_2), Nitrogen Oxide (NO_2), and heavy metals such as Mercury and Arsenic that have been linked to acid rain, smog and health issues [5].On the other hand, syngas combustion has proven to be cleaner compared to coal fired plants. Through integrated gasification combined cycle (IGCC) technologies, the production of cleaner electric power with reduced carbon dioxide emissions is possible. IGCC plants produce 82% less carbon monoxide, 21% less oxides of nitrogen, 71% less sulfur oxide, 66% less mercury , 97% less fluorides, 90% less sulfuric acid mist , and 58% less particle matter. [6] The pollutant emissions discussed here will be further elaborated on in Chapter 2 of this thesis.

1.4   Alternative Fuel Sources

Due to its environmental impacts and as part of the President Obama's Climate Action Plan, the U.S. Environmental Protection Agency (EPA) has released regulations for carbon emissions from new-coal fired and gas fired power plants [5].

> "Climate change is one of the most significant public health challenges of our time. By taking commonsense action to limit carbon pollution from new power plants, we can slow the effects of climate change and fulfill our obligation to ensure a safe and healthy environment for our children," *EPA Administrator Gina McCarthy*

These new standards drive innovation to design the next generation of power-plants gas turbines that will create a more sustainable clean energy economy. The need to meet these challenges increases the necessity to find alternative flexible fuel sources that produce fewer emissions.

Integrated Gasification Combined Cycle (IGCC) plants are a good example of new technologies that aim to solve the current challenges associated with coal and its emissions. IGCC plants create synthetic gas, also known as syngas, by taking coal through a gasification process. IGCC plants us different processes in order to gasify coal, extract ad sequestrate CO_2 and recuperate other chemicals such as sulfur and N_2.

Syngas is ideally a mixture of hydrogen and carbon monoxide produced by gasifying a solid fuel feedstock such as coal or biomass. There are multiple products such as CH_4 and tars of aside carbon monoxide and hydrogen in the production of syngas .The gasification process is carried out by using the heat from carbon oxidation to sustain the gasification reaction and the fuel is mixed with an oxidant, such as air or oxygen, to gasify the fuel [6].

1.5   Flame Characteristics

A flame is a self-sustaining propagation of a localized combustion zone at subsonic velocities [4]. It is essential to understand syngas flames properties. Such properties determine the behavior of the flames. The study of combustion requires an understanding of the fundamental combustion properties of these mixtures since it assist in the design of efficient fuel-flexible injectors and combustors [6] . Flames can be characterized by the way they are mixed such as diffusion flames and premixed flames, a brief description of these different types of flames are descried in the following sections.

1.5.1   Diffusion Flames

In a diffusion flame, also known as non-premixed flame, the reactants are initially separated and the reaction occurs only at the interface between the fuel and the oxidizer where both mixing and reaction take place [4]. These types of flames will not be thoroughly discussed in this thesis since the work presented here involves the combustion of premixed-gases.

4

1.5.2 Premixed Flames

In a premixed flame the fuel and the oxidizer are mixed in a molecular level prior to the occurrence of any significant chemical reaction [4].

Premixed flames combust cleaner, in terms of pollutant emissions, and are more efficient compared to diffusion flames since it is possible to control the input of the fuels and oxidizers mixed before combustion. However, premixed flames introduce safety issues such as flashback, lift off, and blowout conditions. All the issues related with the use for premixed flames are influenced by the flame speed, chemistry, equivalence ratio, pressure, and temperature of the fuel –air mixture.

Premixed flames can be categorized by their adiabatic flame temperature, flame structure, flame thickness, and flame propagation or flame speed.

Figure 1 illustrates the main differences between a diffusion flame and a premixed flame
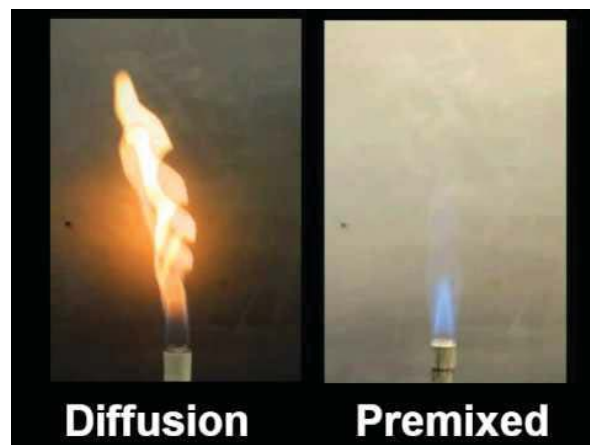
Figure 1- Diffusion and premixed flame [22]

1.5.3 Flame Speed

The fundamental parameter that characterizes flame propagation in a premixed reactant mixture is the laminar flame speed. An anchored or stationary flame is achieved when the local velocity normal

to the flame equals the flame speed. Flame speed is a very important characteristic a fuel mixture since it is relevant determining the flashback and blowout velocities of any given burner .

Flame speed is highly influenced by the presence of hydrogen in syngas. The ratio of hydrogen and carbon monoxide determines the flame speed of the syngas flame during combustion.

Figure 2 illustrates an equivalence ratio vs. flame speed graph at various H_2/CO fuel compositions. Notice the flame speed change as the hydrogen concentration increases in the fuel mixture.
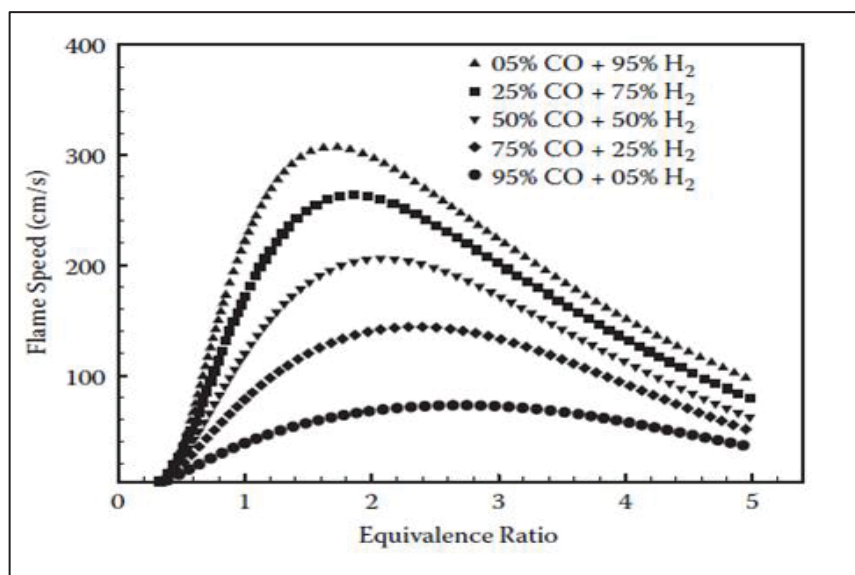
Figure 2- Equivalence ratio vs. Flame speed for various syngas compositions [6].

1.5.4 Flashback

Flashback is a condition in combustion that causes a premixed flame to propagate upstream against the gas stream [4]. Flashback is a safety hazard since it can cause substantial hardware damage, denotations as well as increasing pollutant emissions. In premixed lean flames flashback occurs due to one of the following reasons: (i) Boundary later flame propagation (critical velocity gradient), (ii) Turbulent flame propagation in core flow, (iii) Combustion instabilities, and (iv) Upstream flame propagations induced by combustion induced vortex breakdown (CIVB) [7].

Figure 3 illustrates the flashback phenomenon in detail. Flashback occurs when the flame speed, S_L, is greater that the velocity of the gas velocity flow through the glass tube.
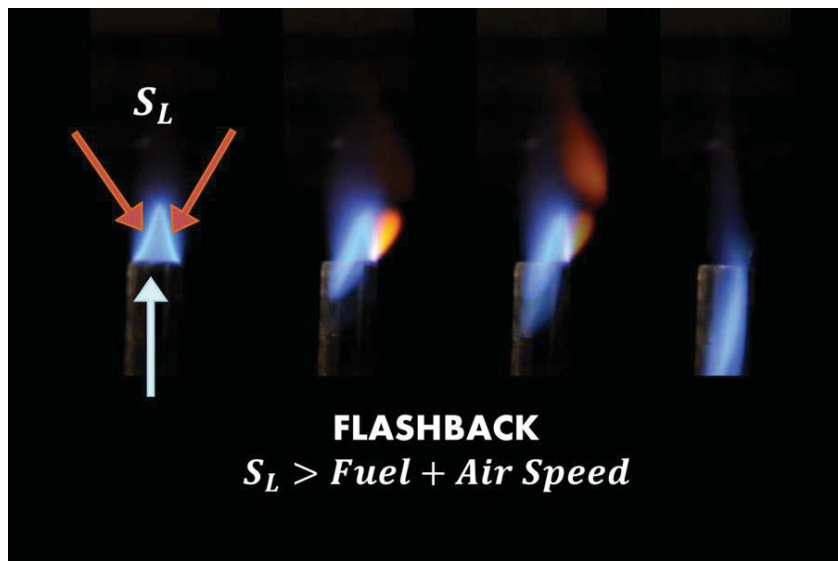
Figure 3- Flame flashback in a glass tube. Based on [23]

Flashback propensity is dependent in flame speed, pressure, temperature, and fuel composition. For example, the presence of hydrogen in syngas significantly increases the potential for flashback. Due its high laminar burning velocity and low lean flammability limit, the presence of hydrogen in syngas tends to shift the combustion to flashback operating conditions [7].

7

1.5.5 Flame lift-off

An important design criterion for gas burners is the avoidance of liftoff. A lift-off condition is characterized when the flame is no longer attached at the burner port or tube rather it is stabilized at a distance from the port. Flame lifting is generally undesirable due to its contribution to some escape of unburned gas or incomplete combustion as well as its difficulty to achieve ignition above the lifting limit [4].

Flame lifting depends on local flame and flow properties near the edges of the burner port. A flame is considered to be attached when the edge of the flame near the burner lip [4].

1.5.6 Flame blowout

When the velocity of the gas is increased and the edge of the flame is displaced from the burner tip, the flame is in a lift-off condition. As the velocity of the gas further increases, it results in an increase of the lift off distance until the flame blows off of the burner. This flame phenomenon is known as blowout and it is an undesirable condition. Both lift off and blowout is caused by the effects of decreased heat and radical loss to the burner tube as well as increased dilution with ambient fluid [4]. Blowout phenomenon can be detailed observed in Figure 4.
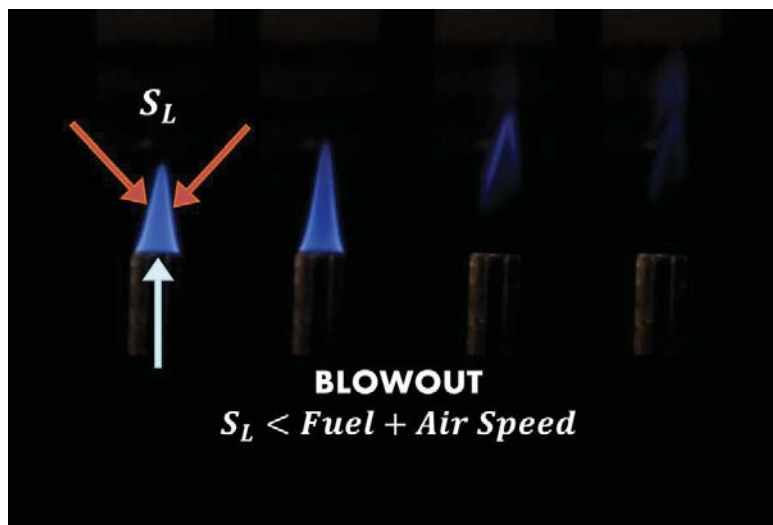
Figure 4- Flame blowout in glass tube. Based on [23]

1.6   Objective

The main objective of this thesis is to improve flame stability to reduce NO pollutant emissions from a gas turbine combustor. To meet this goal this study will first test and determine the flame stability limits of a previously designed multi-tube fuel injector. The injector will operate using various syngas concentrations in a high-pressure combustor. Multiple experiments will be performed in order to assess and better understand the behavior of the flame emitted from the injector. All tests will be conducted in a high-pressure combustor rig. In order to meet the objective of this project, the following tasks will be carried out:

1. Create a stability map by performing multiple experiments with the existing multi-tube fuel

2. After testing, provide design improvements to the existing multi-tube fuel injector in order to further increase flame stability.

1.7   Practical relevance

The testing of a previously designed multi-tube fuel injector will lead to a better understanding of flame stability of syngas at various compositions and equivalence ratios. Various syngas combustion and flame characteristics such as flame stability, flame velocity, flame propagation, flashback and blowout propensity will be examined. The experimentation and data obtained by the multi-tube fuel injector will increase the knowledge of combustion of syngas and will support the development of the next generation combustion systems.

Chapter 2: Literature Review

This chapter will present a detailed overview of previous and current research. It is important to study and understand earlier and ongoing investigations in order to have a reference baseline and being able to compare empirical and experimental results of systems operating at similar conditions. Chapter two illustrates a background in the area of high-pressure combustion, flame stability and new methods to achieve flame stability as well as low combustion emissions. Also, this chapter will present the current research in the high-pressure combustor used at Center for Space Exploration Technology Research (cSETR) laboratories of The University of Texas at El Paso (UTEP).

2.1   High Pressure Combustion

High-pressure combustion research is an important topic of study since the combustion kinetics and reaction rates of fuel combustion change at high pressures when compared to ambient combustion. Combustion at high pressure occurs in gas turbines. Gas turbines can be found in power plants and airplane turbines among others. Gas turbine combustors of advanced power systems have the goal to operate under specific conditions such as fuel variability, fuel flexibility, and they must operate in such way that low pollutant emissions (NO_x < 2ppm) are achieved [8]. Developing an understanding in high-pressure combustion is important since it will aid in the development of modern combustion devices. The future generation of gas turbines should be design in such way that they can tolerate various types of fuels such as syngas in various concentrations, and natural gas [9].

High-pressure combustors for research purposes are currently operated in various parts of the United States and around the world. An example of this is Cambridge University High Pressure Combustion Lab. Cambridge University designed and developed an optically accessible combustor that is capable to operate up to 600 °C and 1 MPa and up to 0.9 kg/s [10].

The University of California Irvine Combustion Laboratory (UCICL) has performed research in a high-pressure combustion chamber for over 30 years. UCICL has two fully operation high-pressure combustors, a high optical access facility, and a combustor designed for duration tests [11].

The Center for Space Exploration Technology Research (cSETR) laboratory at the University of Texas at El Paso currently performs research in the area of combustion. The facility has both modular optically accessible ambient and high-pressure combustors. Both combustors have been extensively used to increase the understanding of syngas combustion.

The high-pressure combustor (HPC) at the University of Texas at El Paso is designed to operate at a pressure up to 1.5 MPa and can handle a temperature of up to 2400K. The combustor system was designed in such way that it can withstand the combustion effects of high hydrogen content fuels. The air mass flow rate capabilities of the combustor are to set to a maximum of 81.93 g/s. Syngas fuel (H_2-CO), with up to 30% of hydrogen concentration, can be used in the combustor with a maximum flow rate of 35.77 g/s.

The HPC is a modular system composed of 4 primary modular sections:

    i.   Inlet static mixed

   ii.   Inlet cap

  iii.   Optically accessible combustion chamber,

  iv.   Variable exhaust throat area restrictor

         a.   Composed of a converging nozzle and exhaust

The combustion chamber is equipped with 3 quartz windows in order to observe the internal reactions of the combustion as well as the behavior of the various burners that will be tested in this system. Figure 5 illustrates the CAD design of the optically accessible high-pressure combustor at the cSETR.
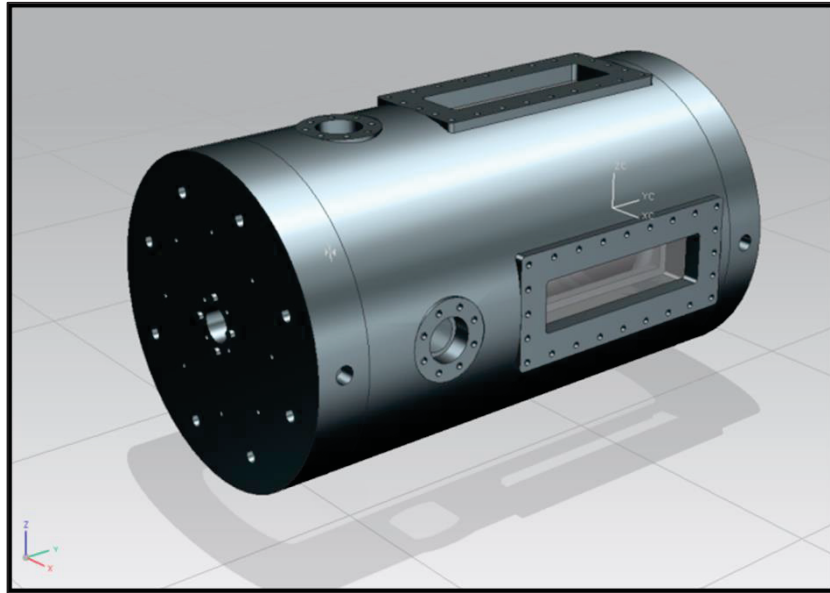
Figure 5 - Optically accessible High Pressure Combustor CAD model [10].

2.2   Gasification Processes

The use and production of syngas or 'town gas", as it was referred in the past, dates back to the 1800s. Interest in syngas technologies has increased as the demand of alternative energy sources has grown in the last 10 years. The main reasons why syngas production is of great interest is because it can be generated from solid fuel feedstock such as coal which is abundant in the United States. Also, syngas can be used as a fuel for power generation, fuel production, and chemical manufacturing. Syngas production possesses the ability to separate CO_2 for geological sequestration.

Gasification is the process in which coal or any feedstock is converted into syngas. This process uses the heat of carbon oxidation to maintain the reaction by mixing the coal or feedback with an oxidizer that can be air or oxygen depending on the application. Water is used to control the temperature of the gasification reaction. As previously mentioned in Chapter 1, syngas is a mixture of hydrogen and carbon monoxide in its final stage, however, after gasification syngas includes various products such as CH_4, CO_2 and tars. Syngas is then post-processed and cleaned in order to produce compounds of sulfur, nitrogen, chlorine, and mercury among others. Figure 6 illustrates an example of gasification process and its major reactions [6].

12
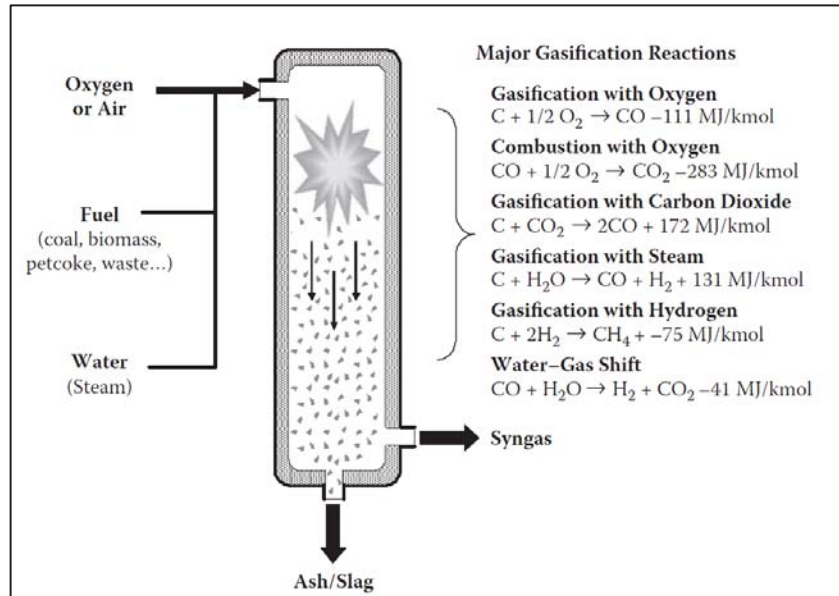
Figure 6 - basic gasification process and its major reactions [6].

2.2.1 Moving Bed Gasification

The moving bed gasifier can be found in two different arrangements: updraft and downdraft. In updraft of counter-flow gasifiers coal enters the reactor from the top whereas the oxidizer enters from the bottom. On the other hand, in the downdraft or co-current gasifiers the coal and oxidizer enter the reactor together. The high temperature produced in the co-current gasifier help to complete the gasification reactions to produce syngas with low tars concentration, however the gas must be integrated in downstream processes in order to achieve overall efficiency due to its high sensible heat. Counter-flow produces high temperature which allows rapid consumption of coal. The hot gas in the counter-flow process moves upward passing through the fuel source which helps to cool down the gas. Various compounds such as tar and oxygenated particles are formed in syngas due to its low temperature. Such compounds must be removed in the clean-up processes. Figure 7 illustrates both updraft and downdraft gasifiers [6].
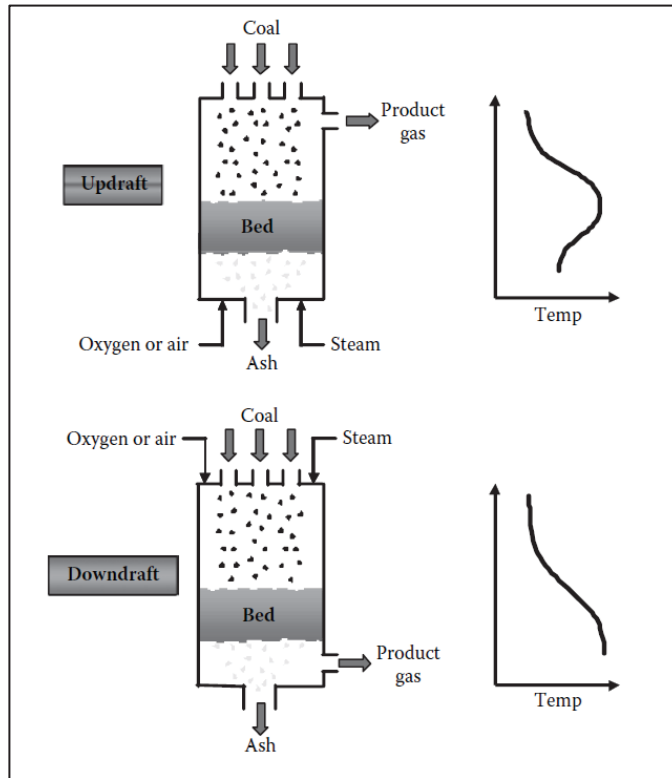
Figure 7 - Updraft and Downdraft gasifiers [6]

2.2.2 Fluid Bed Gasification

Fluid bed gasifiers can be sub-divided into three categories that are characterized by its bulk velocity through the bed.

Bubbling Bed

This gasifier exerts a velocity below 5 m/s and it behaves like a boiling fluid. Due to its low velocity, the temperature is homogenous throughout the coal bed. This even temperature distribution allows the coal to gasify as it leaves the ash bed. Figure 8 shows a bubbling bed gasifier [6].
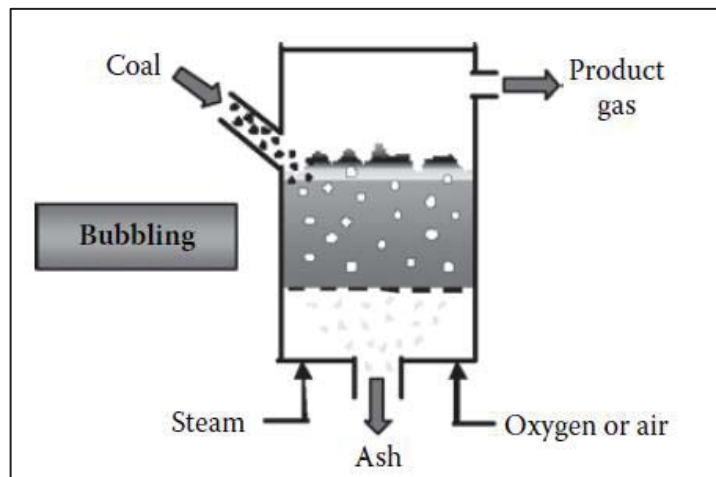
Figure 8 - Bubbling bed gasifier [6]

Circulating Fluid Bed

Due to the increase of its velocity between 5 to 8 m/s, circulating beds allow a better carbon conversion and a lower tar production. The higher velocity increases the coal heating rate and it allows a separation of larger coal particles which are later oxidized. This gasifier can accommodate a greater amount of coal compared to bubbling bed gasifiers [6].
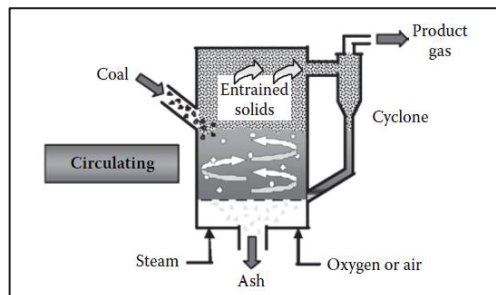
Figure 9 - Circulating bed gasifier [6].

Transport Reactor

This gasification process is used for low-rank coal. Compared to the bubbling and circulating gasifiers, this reactor has a high gas velocity of approximately 15 m/s. Due to its high velocity particles are separated and travel through the reactor and are collected in a stand pipe. After being collected in the

15

stand pipe, the particles are entrained in the system where they go through another cycle of gasification. The transport gasifier has the greatest throughput [6]. Figure 10 sketches a typical transport reactor.
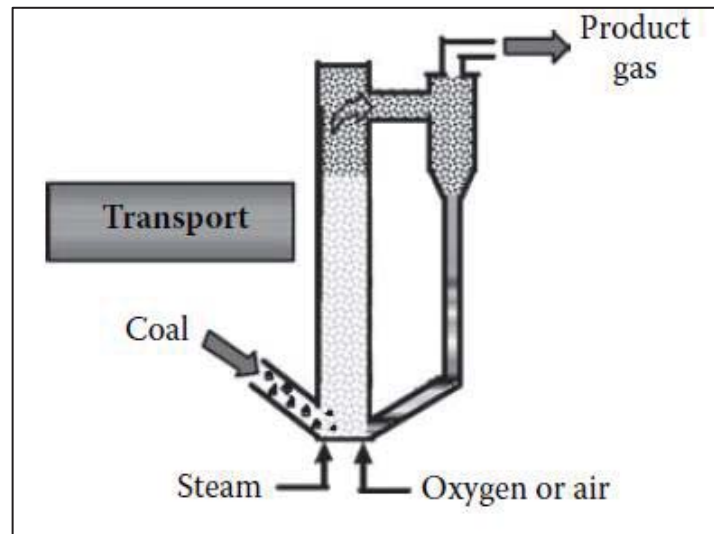
Figure 10 - Transport gasifier [6]

Entrained Flow

Entrained flow gasifiers operate at high temperatures which allow them to melt the coal ash (>1250 °C). Such temperatures are achieved by using a greater amount of oxygen in the combustion process inside the reactor. By using higher temperatures coal is converted to syngas in an efficient way and ensures that the gas is free of tars. Due to its high efficiency IGCC plants have incorporated this type of gasifiers [6]. Entrained flow gasifiers and be down flow and up flow in both single and two stage.

16
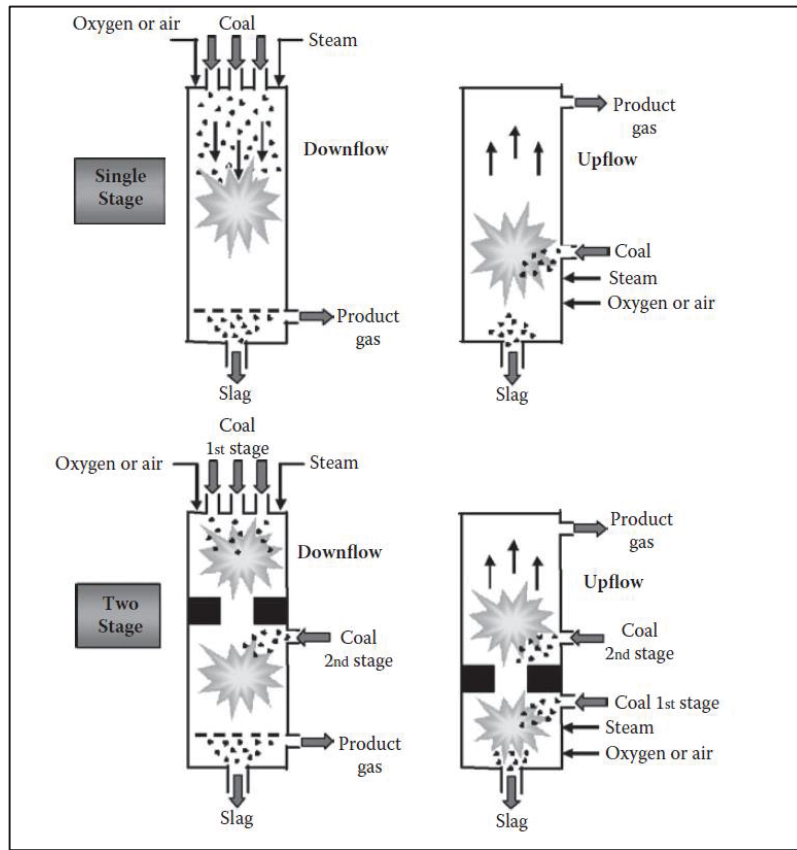
Figure 11 - Entrained flow gasifiers; down flow and up flow [6]

2.3   Syngas Post-Processing

After gasification, syngas contains various products in its gas besides H_2 and CO. Syngas passes through a purification process where impurities are removed, CO_2 is sequestrated and H_2-CO is then moved to gas turbine where it is used to produce energy.

2.4   Combustion Stability

Combustion stability is a topic of high interest since it is imperative to establish an operational window where combustion occurs efficiently. As discussed in previous chapters, phenomena such as flashback and blowout are flame conditions that affect combustion performance. Other issues associated

with combustion operability are combustion instabilities, and auto ignition. Fuel composition is the main cause of such instabilities [6].

2.4.1 Flashback

Flashback is a combustion problem in premixed combustion where the flame propagates upstream towards the steam the premixed gas. Flashback is considered the main operability issue associated with the use of lean high hydrogen content fuels [12]. This phenomenon can cause considerable damages to the equipment of the premixed zone as well as increase pollutant emissions [13]. From all combustion instabilities issues flashback is the most dangerous since it can cause serious hardware damages.

Flashback can be caused by one of the following causes:

-      Flame propagation in the boundary layer
-      Turbulent flame propagation in the core flow
-      Violent combustion instabilities
-      Combustion Induced Vortex Breakdown

The experiments carried at the University of Texas at El Paso by Dam et al [13] were performed using a modular laboratory atmospheric scale gas turbine combustor. The combustor set-up consist in an (i) inlet manifold with a static mixer, (ii) a swirl burner with a mixing tube, and an (iii) optically accessible combustion chamber. The chamber is optically accessible in such way that a High Speed imaging system as well Particle Image Velocimetry (PIV) can be used in order to observe the flashback phenomena inside the combustion chamber [13].

Dam et al. [13] found that CIVB flashback is determined when the flame moves upstream from the tip of the swirler center body to its base due to the formation of recirculation zones around it.

Dam at al. [7] investigated flashback propensity due to hydrogen concentration in a typical syngas mixture, external excitation, critical velocity gradient, and flashback behavior of hydrogen-carbon monoxide and hydrogen-methane mixtures. The critical velocity gradient (g_f) was implemented

in order to measure the flashback propensity of various syngas mixtures. The increase of hydrogen causes a non-linear increase in g_f values. It was demonstrated that the increase of hydrogen even by 5% increases the propensity for boundary layer flashback. Finally, experimental result showed that external excitation does not play a dominant role for syngas mixtures with a hydrogen concentration of 5% or greater [7].

Through experimentation, Daniele et al. [14]found that flashback propensity is mainly dependent in pressure and inlet temperature, however, inlet velocity dependence showed weak results [14]. The set-up where the experiments were performed consisted in a high pressure combustor capable to operate up to 30 bar, with a maximum air flow rate of 1200mn^3/h and an adiabatic flow temperature of 2000 K. This high pressure combustor has the ability to preheat inlet air electrically up to 823K which allows testing for inlet temperature flashback propensity [14]

According to Daniele et al. [14], velocity does not show to present a high influence in flashback propensity. Figure 12 presents data of flashback propensity at various conditions. It can be observed that the circles (T_o=577 K and U_o=45m/s) and diamonds (T_o=577 K and U_o= 60m/s) dependence relies more in the pressure rather than the inlet velocity. Increasing the inlet velocity to avoid flashback can be a good approach; however it has shown little effectiveness as pressure increases [14].

Pressure has a strong influence in flashback propensity. The increase of pressure in the combustion chamber has shown to narrow the operational window of syngas combustion. The turbulent flame speed increases as for equivalence ratios close to flashback at high pressures [14]. Figure 12 illustrates how pressure influences flashback propensity.
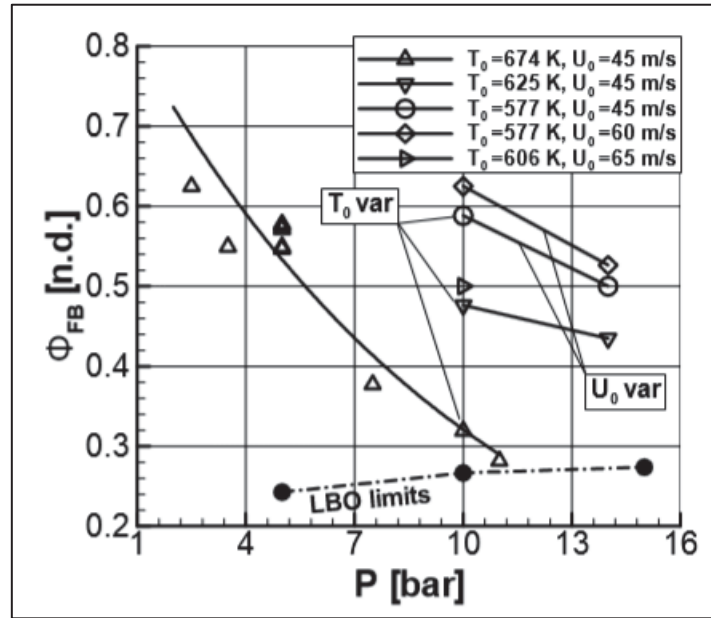
Figure 12 - Flashback dependency on pressure increase

According to Noble et al. [15] during his experiments aimed to find flashback and lean blow limits upon fuel composition, the percentage of hydrogen present in the fuel mixture with a hydrogen mole fraction less than 60% has less effect in flashback characteristics. Both flashbacks due to boundary layer and due to the movement of the static flame position upstream along the center-body have been observed to appear at high and low hydrogen concentrations [16].

Shafer et al. [12]performed experiments using a quarts tube burner which allowed them to visualize the effects of hydrogen concentration in flashback propensity of syngas. Constant adiabatic flame temperature of 1700 K and 1900K were used to determine flashback at various flame compositions of hydrogen, carbon monoxide and methane mixtures. The mixture equivalence ratio was maintained constant while airflow was reduced until flashback occurred. Experimental results showed that flashback is affected by the burner tip temperature [12].

Shafer et al. [12] concluded that flashback occurs in the boundary layer and turbulent conditions lead to lead to variability in the physical location of flashback. Also, higher concentrations of hydrogen increase the propensity of flashback, however, the addition of methane or carbon monoxide aids to inhibit this phenomenon [12].

20

2.4.2 Blowout

Flame blowout also known as the "static stability" limit in a combustor refers to a combustion stage at which the flame detaches from its anchored point and it physically blow out. Blowout occurs when the time required for the chemical reaction is greater than the combustion zone residence time [17]. In other words, the velocity of the fuel and oxidizer mixture exiting the combustion zone is much greater than the flame speed of the mixture itself; hence the flame cannot be sustained under such conditions.

Various combustor blowout characteristics using quasiempirical and physical correlations have been extensively studied [17]. According to Noble et al. [15], blowout limits can be correlated to a ratio of chemical kinetic time and resident time. Such correlation can be then described with the Damköhler number as follows:

$$Da = \frac{\tau_{res}}{\tau_{chem}} = \frac{S_L^2 d}{\propto U_{ref}} \qquad (1)$$

Where τ_{res}/τ_{chem} denote the ratio between the chemical kinetic time and residence time, S_L denotes laminar flame speed, α is thermal diffusivity, d and U_{ref} represent a characteristic length and a velocity scale, respectively. Despite their disadvantages, Damköhler number scales have proven to be a good measure to predict blowout trends for various fuel compositions including $CO/H_2/CH_4$ fuel blends. The results of the experiments performed show that blowout propensity occurs at a constant Da value of 0.6 [15].

The experiments conducted by Noble et al. [15] Were obtained testing a variety of fuel compositions, burned flow velocity, reactant temperature up to 470 K and combustor pressures up to 4.4 atm.

Daniele et al. [16]presented a detailed study of lean premixed combustion lean blow out limits at gas turbine relevant conditions. The experiments carried in this investigation involved preheating temperature up to 772K and pressure up to 1.5 Mpa while various inlet velocities were used [16]. The experiments presented in Daniele et al. [16] work were carried using a high-pressure combustor with complete optical access. The high-pressure combustor system is capable of operating up to a pressure of 3 Mpa, with a maximum mas flow rate of 0.3 kg/s and an adiabatic flame temperature of 1950K. The

21

system is capable of preheating the inlet air up to 823K and it can produce a thermal power of 400 kW [16].

A lean blow out limit can be explained as the point in which oscillations characterized by high amplitude and low frequency appear during the combustion process. Lean blow out limits were detected by OH Chemiluminescence signal acquisitions by means of a high frequency photomultiplier which permits the identification of lean low out before it occurs. Experimental results showed that by increasing the concentration of H_2 in the fuel mixture it is possible to increase the combustion range at leaner equivalence ratios [16].

2.5   Flame Stability Measures: Swirlers

The current turbine combustors burners operate at lean fuel conditions and use various types of swirlers. Swirl burners help to achieve good combustion conditions by providing good fuel and oxidizer mixing well a long residence time which ultimately leads to a complete reaction. However swirlers present a number of concerns such as flashback and blowout [13].

Noble et al. [16] noted that classical flashback scaling result from Bunsen flames experiments do not have a relevant to study parameter regimes found in swirler burner flames

Combustion Induced Vortex Breakdown has been demonstrated to be the main cause of flashback in swirl burners. CIVB flashback exists in instabilities of its vortex core which are controlled by Swirl and Reynolds numbers [18].

Dam et al. [13] performed various experiments in order to establish the flame flashback limits of swirl burners using various H_2-CO mixtures as well as actual syngas compositions. In order to compare the effect of burner configuration, two center body swirlers were used, the first one with six vanes and swirl number 0.71 and the other one with 12 vanes and swirl number 0.97. High swirl numbers tend to cause turbulent flame propagation in the core flows [13].

2.6   Flame Stability Measures: Multi-tube Injector

Although swirlers are widely used in industry and gas turbines for combustion due to their good mixing characteristics as the fuel mixtures passes through its vanes, the design, development and testing of multi tube fuel injectors has been recently studied with the main purpose of finding alternatives that will help to reduce NO_x emissions as well as to decrease flashback propensity.

York et al. [19] developed and tested a fuel injector designed specifically for low-NO_x combustion in high concentration fuels such as syngas. The fuel injector was designed with jet-in-cross flow mixing of the fuel and air aside of multiple small diameter tubes across the injector face. This multi-tube fuel injector was tested in a small scale single nozzle rig using high pressure gas turbine conditions. Flashback free operation was observed for a fuel mixture of 60%H_2 and 40% N_2 and temperature over 1900K. Although this injector is capable to operate without flashback, its NO_x emissions were higher compared to a perfectly mixed experiment utilizing the same fuel composition [19]. Figure 13 illustrates a large-scale multi tube mixer used for high hydrogen content fuels.
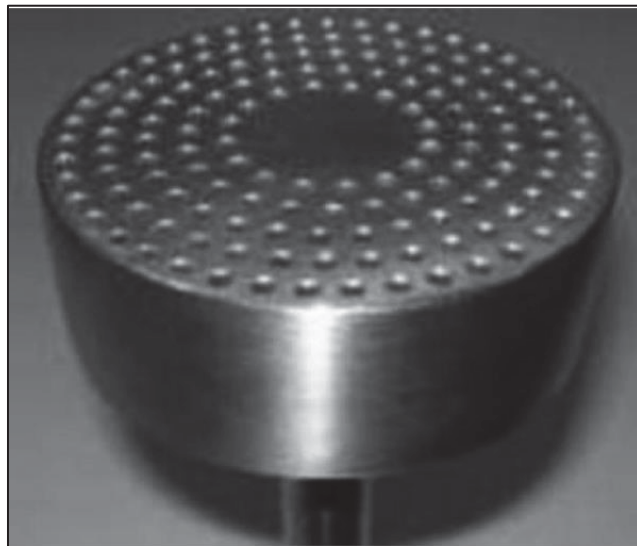
Figure 13 - Multi tube mixer [19].

Hollon et al. [20] was able to achieve the program goal of 2ppm NO_x emissions at adiabatic flame temperature of 1750K and 50% hydrogen concentration fuel by utilizing a mixing cup consisting of small size and rapid mixing port that ensure the proper mixing of fuel and air at the cup exit. This

23

micro-mixing lean premixed system was designed to operate at fuel mixtures from 100% natural gas to 100% hydrogen. The Parker micro mixing cup use is promising for future gas turbines as it can operate flashback free. Figure 14 shows the Parker micro mixing cup configuration [20].

Figure 14 - Parker mixing cup [20].

Chapter 3: Experimental Set-Up

3.1 High Pressure Combustion Testing Facility

The Center for Space Exploration Technology Research (cSETR) Laboratory at The University of Texas at El Paso (UTEP) designed and developed a high-pressure combustor facility aimed to research and understand combustion of high hydrogen content fuels, such as syngas, at high pressures. This testing facility is capable to study flame stability, various fuel injection methods and analyze combustion emissions such as CO_2, CO and NO_x.

The high-pressure combustor is conformed of 4 main modular parts and an automated control system: (i) Inlet manifold with static mixer, (ii) inlet cap, (iii) optically accessible combustion chamber, (iv) variable exhaust throat area resistor and (v) automated flow control system. Figure – illustrates a detailed view of the high-pressure combustor system that operating in the cSETR facility at UTEP.
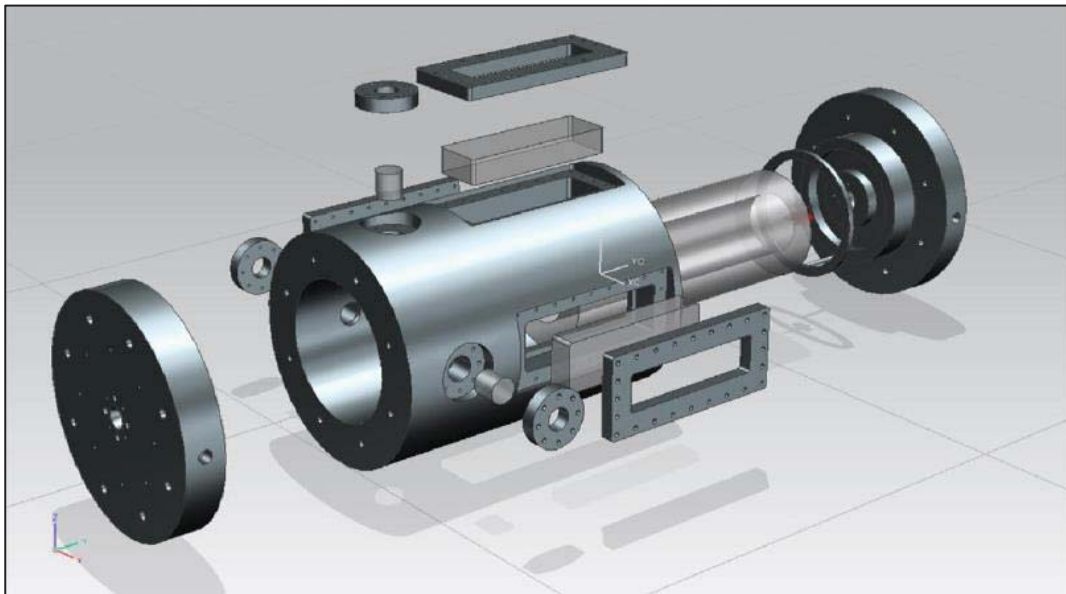
Figure 15 - High pressure combustor laboratory set-up at cSETR UTEP

The inlet manifold mixes the mixture of fuel and oxidizer before it enters the combustion chamber. The inlet manifold is composed of 3 sections:

    a. Inlet manifold (Fuel/Oxidizer mixer)

    b. Static mixer

c. Combustor connector

The fuel/oxidizer mixer consists of fuel-oxidizer injection system which main objective is to introduce the gases into the system and mix them before the gases reach the combustion area. The mixer is composed of 4 tangential injection fuel ports and 1 central port used for the oxidizer. Figure 16 illustrates the fuel and oxidizer mixer of the high-pressure combustion system
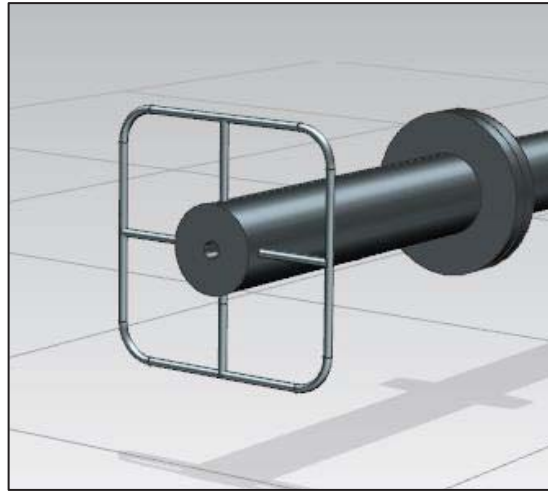
Figure 16 - Fuel/Oxidizer mixer used in cSETR high-pressure laboratory

The static mixer connects via a flange with the fuel/oxidizer mixer and it consist on a honeycomb which is installed downstream the flow which allows the gases to stabilize after they enter the system through the fuel/oxidizer mixer. The honeycomb is has been 3D printed at the W.M. Keck Center of 3D Innovation at the University of Texas at El Paso. A sectioned view of the inlet manifold and the static mixer is illustrated in figure 17. Figure 18 illustrates the honeycomb used inside the static mixer.
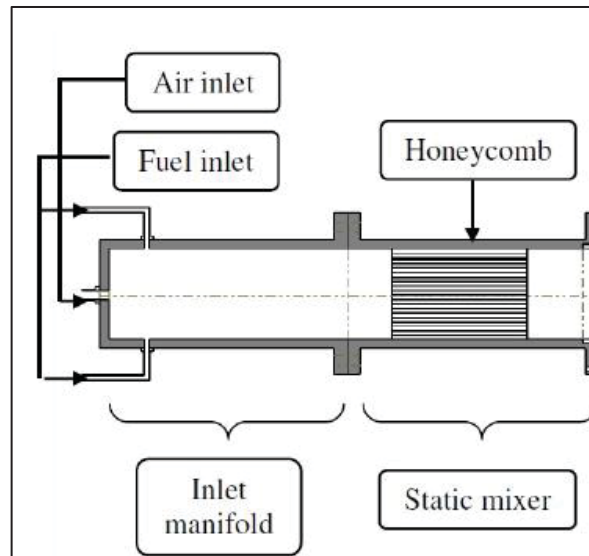
Figure 17 - Inlet manifold and static mixer schematic diagram
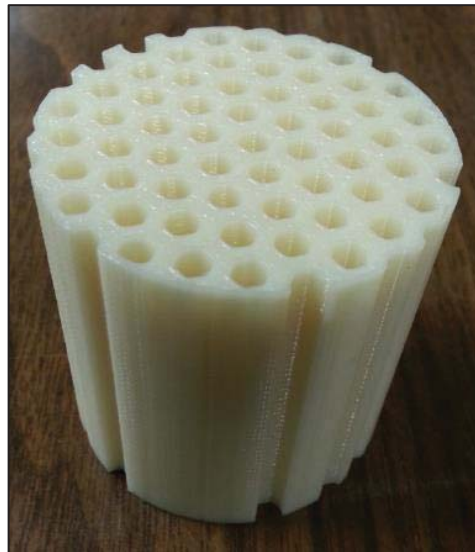
Figure 18 - Honeycomb used in static mixer fabricated by W.M Keck Center for 3D innovation

Finally, the combustor connection is the final flange that connects the fuel/oxidizer mixer, the static mixer and the multi-tube fuel injector to the combustion chamber. The combustor connector is secured with nine bolts that are bolted into the front cap of the combustion chamber.

The inlet cap, optically accessible combustion chamber and the variable exhaust throat in the end cap integrate the combustion chamber set-up. The front cap house the ignition source as well as the

27

multi-tube fuel injector or a swirler burner depending of which experiment is being performed. The optically accessible combustion chamber is where the combustion reactions take place. The chamber is equipped with the squared windows, hence optically accessible, that ease the detailed observation of experiments. The quartz windows in the combustion chamber allow the use of various devices for flame observation and characterization such as video cameras, laser Particle Image Velocimetry (PIV) devices, intensifiers, etc. Also, the chamber is equipped with 3 instrument ports that are designed to be used and modified accordingly to accommodate data acquisition instruments such as pressure transducers and thermocouples among others.

Finally the variable throat exhaust in the end cap allows the system to be pressurized for high pressure combustion testing. The variable throat is a modular unit that can be removed and modified as needed in order to achieve the desired pressure for any given test. When removed, the combustor is capable to operate at atmospheric conditions. Figure 19 illustrates the 3 modular parts of the combustor chamber mentioned above. The front cap in the far left, the optically accessible combustion chamber with the instrument ports in the center and the variable throat exhaust in the far right of the picture.

Figure 19 - Combustion chamber front cap, chamber and end cap.

The high-pressure combustor was designed to be able to handle the following operational specifications. The system must be able with a chamber pressure of 1.5 MPa and operating adiabatic

flame temperature of 2400 K. The material selected of the high-pressure combustion system is stainless steel 410. A table of the mechanical properties of stainless steel 410 is shown below.

Table 1 - Mechanical properties of stainless steel 410.

Mechanical Properties

Typical mechanical properties for grade 410 stainless steels are given in table 2.

Table 2. Mechanical properties of 410 grade stainless steel

Tempering Temperature (°C)	Tensile Strength (MPa)	Yield Strength 0.2% Proof (MPa)	Elongation (% in 50mm)	Hardness Brinell (HB)	Impact Charpy V (J)
Annealed *	480 min	275 min	16 min	-	-
204	1310	1000	16	388	30
316	1240	960	14	325	36
427	1405	950	16	401	#
538	985	730	16	321	#
593	870	675	20	255	39
650	755	575	23	225	80

* Annealed properties are specified for Condition A of ASTM A276, for cold finished bar.

Due to associated low impact resistance this steel should not be tempered in the range 425-600°C

3.1.1 Control System

The high-pressure combustor system is designed to operate with carbon monoxide and hydrogen as fuel, methane as ignition source gas, and air as the oxidizer. A control system was implemented to ensure the effective delivery of fuel gases and oxidizer into the combustion chamber. The hardware in the control system is controlled remotely from a computer using a Lab View block diagram programmed to meet the requirements of the system. The schematic of the delivery system is illustrated in figure 20.
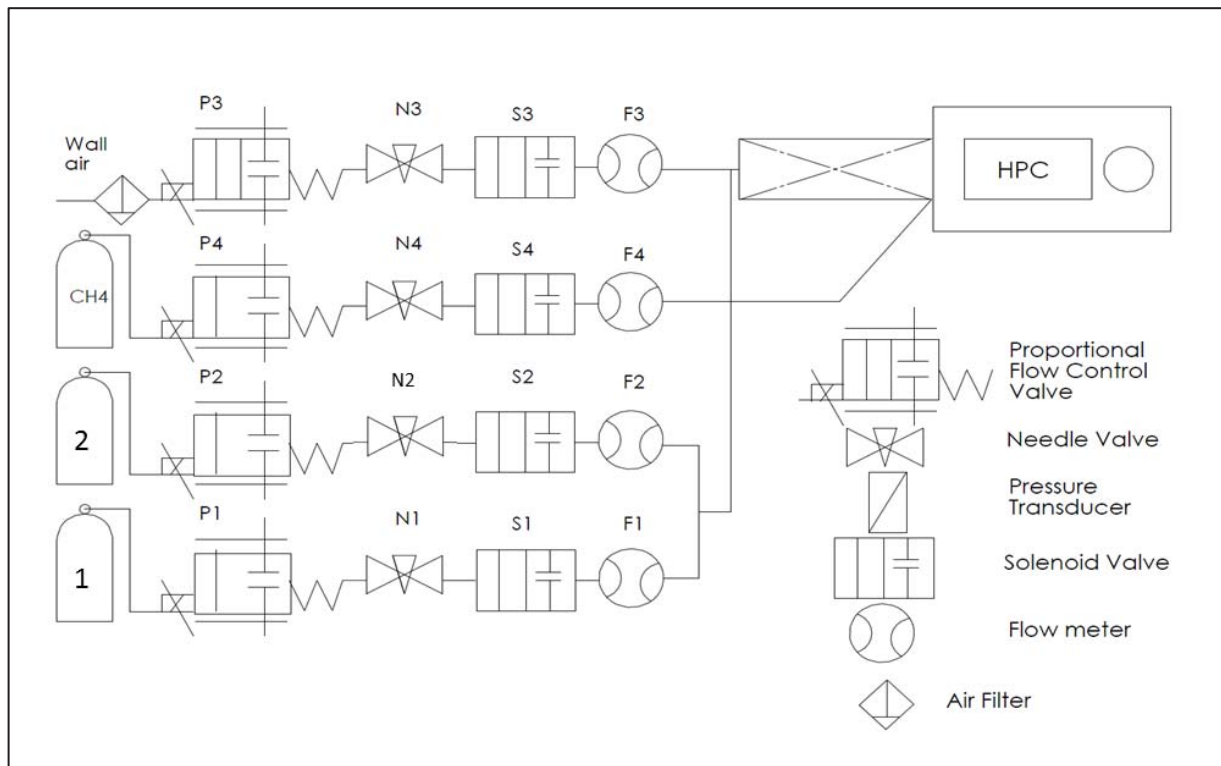
Figure 20 - High pressure combustion system schematic.

The control system hardware consists in proportional valves, solenoid valves, needle vales, flow meters, and ignition coil. The proportional valves operate with a voltage input that controls the amount of flow allowed through the valve. The voltage input is supplied remotely via Lab View interface. The solenoid valves server as a safety measure which is capable to open and close the flow as necessary (i.e. an emergency shutdown). The needle valves act as a fine flow regulators that allows the system to be set-up to a specific flow according to any given test matrix specified. The gas flowmeters show the instant flow of the gas flowing through the device. The flow meters are connected to the Lab View interface and provide real time feed of the current gas flow in the system. The Ignition system consists in a MSD ignition coil and a 12V battery connected to a signal generator and to a spark plug. The ignition system is controlled via Lab View. Figure 21 illustrates a top view of the control system used in the high-pressure combustor system.

30
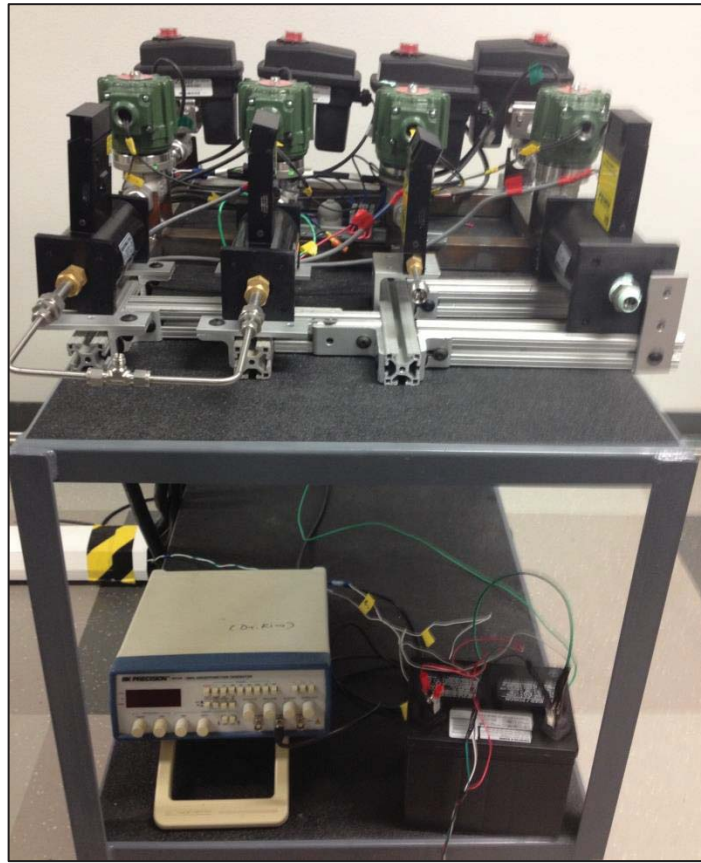
Figure 21 - Hardware control system set-up

Proportional Valves

A set of 4 proportional valves EH2 Series from KZ Valve actuated with a 12 VDC signal and voltage input requirement from 0-10V. These valves are two-way operated by a motor that turns a stainless steel ball valve which regulates the flow as voltage is supplied from the Lab View interface. The valves are rated up to 6895 kPa. Figure 22 illustrates in detail the proportional valves used in the high-pressure combustion system.

Figure 22 - KZ proportional valve EH2 Series

Solenoid Valves

A set of 4 solenoid valves 1314 Series model number 1314IA06T from Jefferson valves have been implanted in the system as a safety measure. The solenoid valves are actuated with a 120 VAC signal and are controlled via a relay card and the Lab View interface. The solenoid valves are illustrated in figure 23.

Figure 23 - Jefferson Valves 1314 Series

32

Flow meters

Various Omega gas flow meters are installed in the system to measure the gas flow in the lines. Omega FMA 1820A – 1840A Series were selected based in their flow capacities (5 LPM – 200 LPM). The flowmeters operate with an excitation voltage of 12 VDC and produce a signal from 0-5 VDC as feedback that can be acquired by Lab View. Figure 24 illustrates an Omega gas flow meter similar to the ones used in the high-pressure combustion laboratory. A detailed description of all flowmeters utilized for the various testing performed in the high-pressure combustion system can be found in Appendix A

Figure 24 - Omega FMA gas flow meter 1700A/1800A Series

Power supply

An EXTECH 382270 and a MASTECH DC power supply was used to meet the power requirements of the various instruments used in the High-pressure combustor control system. Two units provide a total of four power outputs: 0-30V with a maximum current of 5 A., a 3-6.5V with a maximum current output of 3A and an 8-15V with a maximum current output of 1A. The MASTECH DC power supply was used to power the proportional valves. This power source is capable to provide only one power output with variable voltage up to 24 V and a current output up to 10 Amps. Figure 25 illustrates the EXTECH 382270 power supply to the left and the MASTECH DC power supply to the right.

www.manaraa.com

Figure 25 – EXTECH 382270 (Right) and MASTECH DC (left) power supplies.

Ignition System

The ignition system in the high-pressure combustor provides de adequate initial diffusion flame and heat to ignite the hydrogen-carbon monoxide and air mixture for each test. The ignition system consists in a modified spark plug, an ignition coil, a 12 V battery, and a signal generator. These components are interconnected and controlled via a relay card and Lab View interface. The MSD 8287 multi-spark coil illustrated in figure 26 is used to create the necessary energy discharge that is needed for the spark plug. This ignition coil requires a 100Hz frequency as well as a 5V input supplied by the signal generator and the 12 V batteries respectively. The signal generator used in this system is a BK precision 4012A and is shown in figure 27. The overall ignition system is illustrated in both figure 28 and 29 where the battery and signal generator can be observed as well as the final assembly set-up with the front cap of the high-pressure combustor.

34
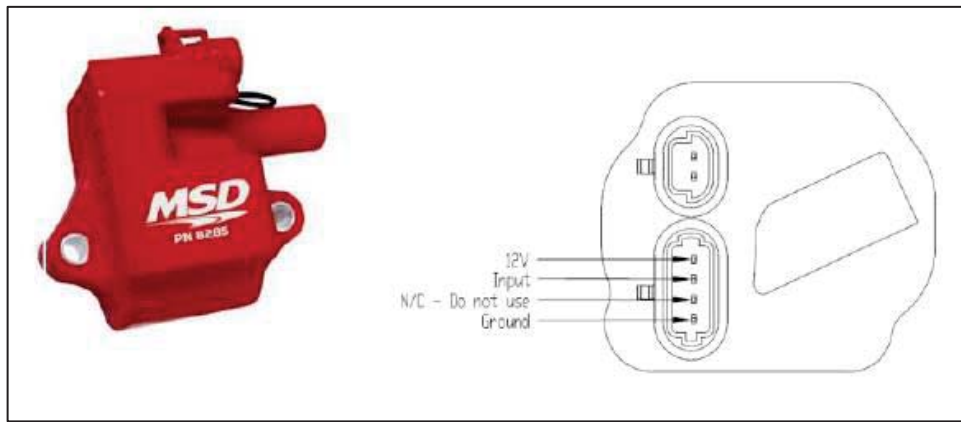
Figure 26 - Ignition coil MSD 8285 and corresponding connecting pin out.

Figure 27 - Signal generator BK Precision 4012A
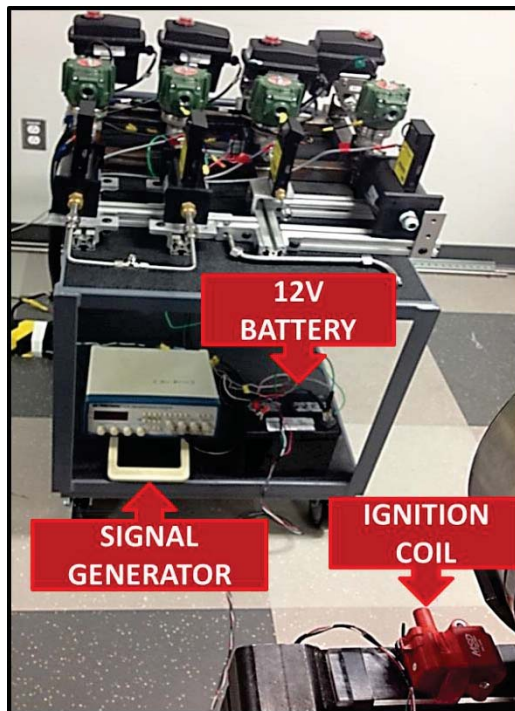
Figure 28 - Ignition system overview

35

Figure 29 - Modified spark plug in ignition system set up

Data Acquisition system and Lab View Interface

The data acquisition system consists of one National Instruments (NI) PCI relay card NI PCI-6521 which has eight mechanical relay outputs and can output up to 150 VAC or VDC. The NI PCI – 6521 illustrated in figure 30 is used to control the solenoid valves, the ignition system and the emergency shutdown. The system is equipped with two NI USB – 6008 data acquisition devices, illustrated in figure 31, used to receive feedback from the flowmeters and the system and they supply 0-5V to the proportional valves.
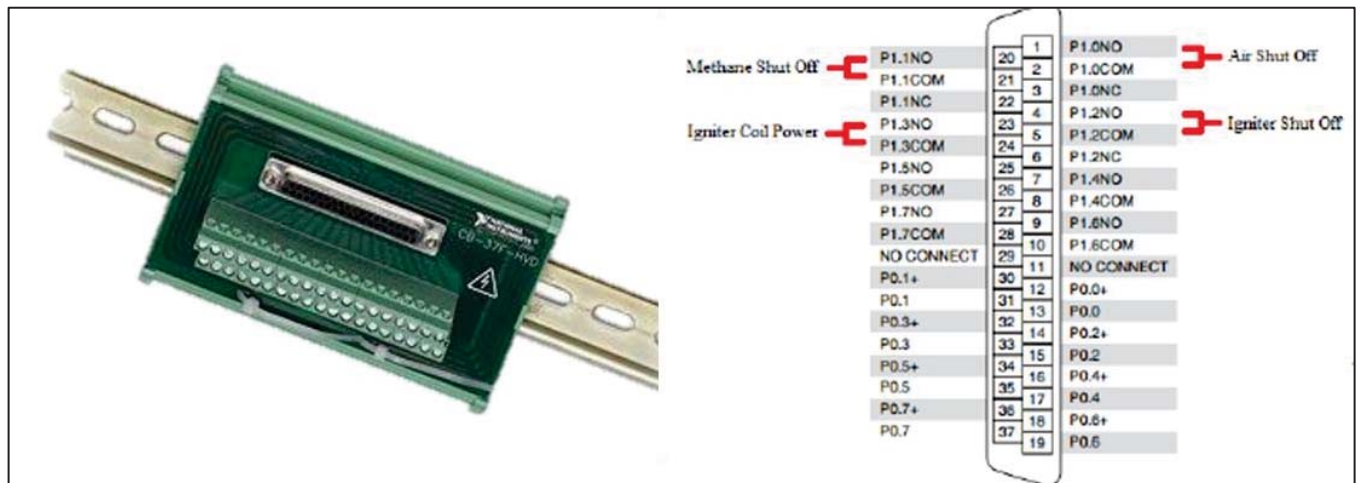
Figure 30 - NI PCI 6521 and pin out assignment
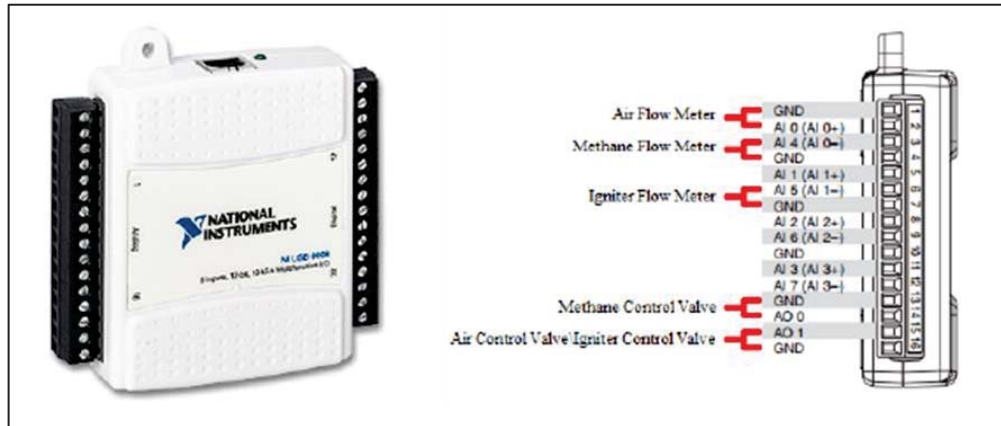
Figure 31 - NI USB 6008 data acquisition device and pin out assignment

The data acquisition system is controlled remotely via a Lab View interface programmed specifically to control the system controls as well as to visualize and record real time data feed from the combustor. Lab view is capable to control the ignition system, the proportional control valves, solenoid valves, and it received data from the flowmeters in the system. An illustration of the Lab View user interface can be appreciated in figure 32.
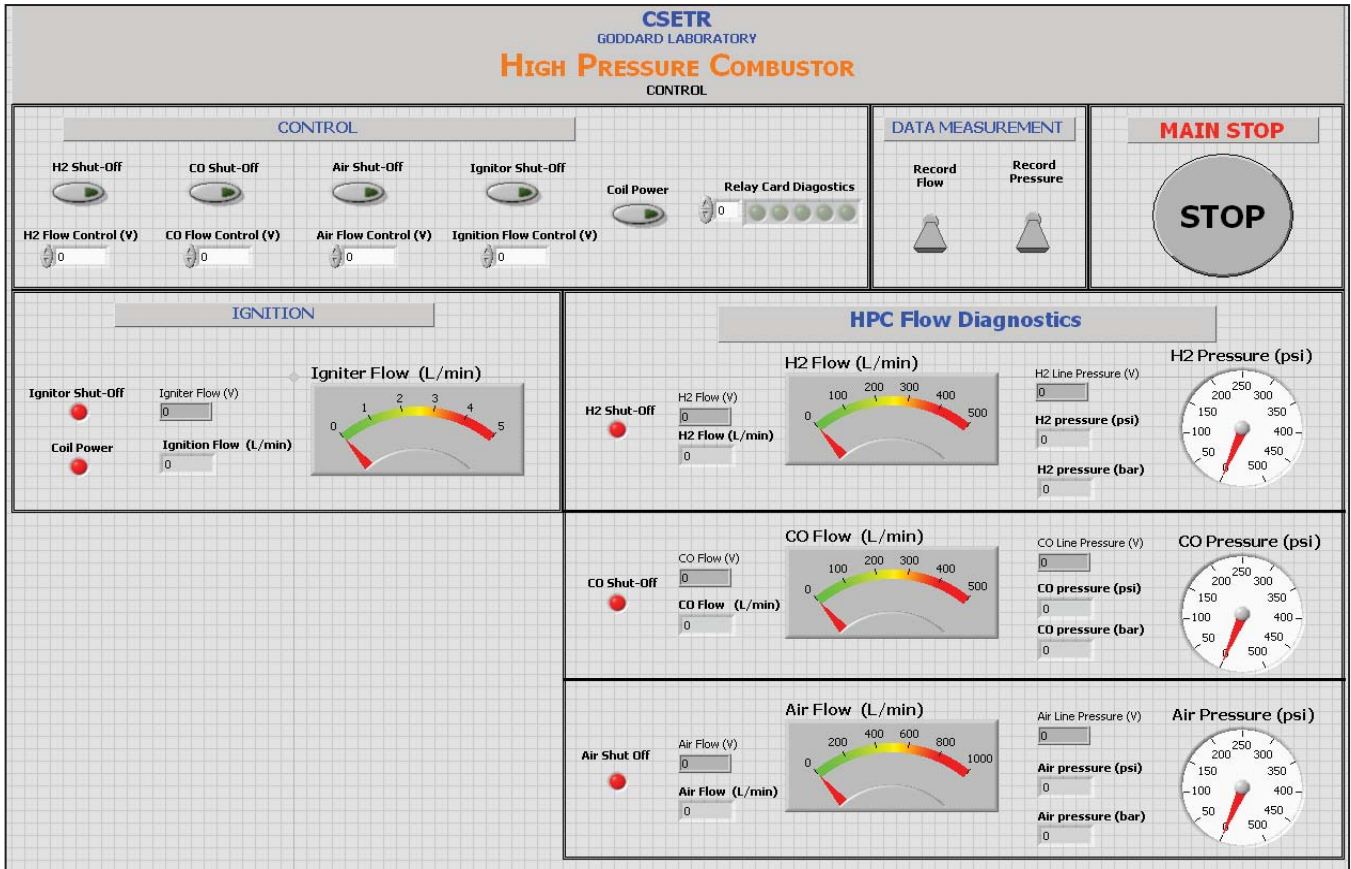
Figure 32 - Lab View user interface used to control the high-pressure combustion system

The user interface was designed in such way that it will give the user the ability to control the system, record data and obtain graphical representation of the behavior of the system under operation. In order to obtain such information it is necessary to create a block diagram in Lab View where calibration data corresponding to a given instrument is input to obtain the desired information output from the system.

38

Figure 33 illustrates the block diagram for the high-pressure combustion system.
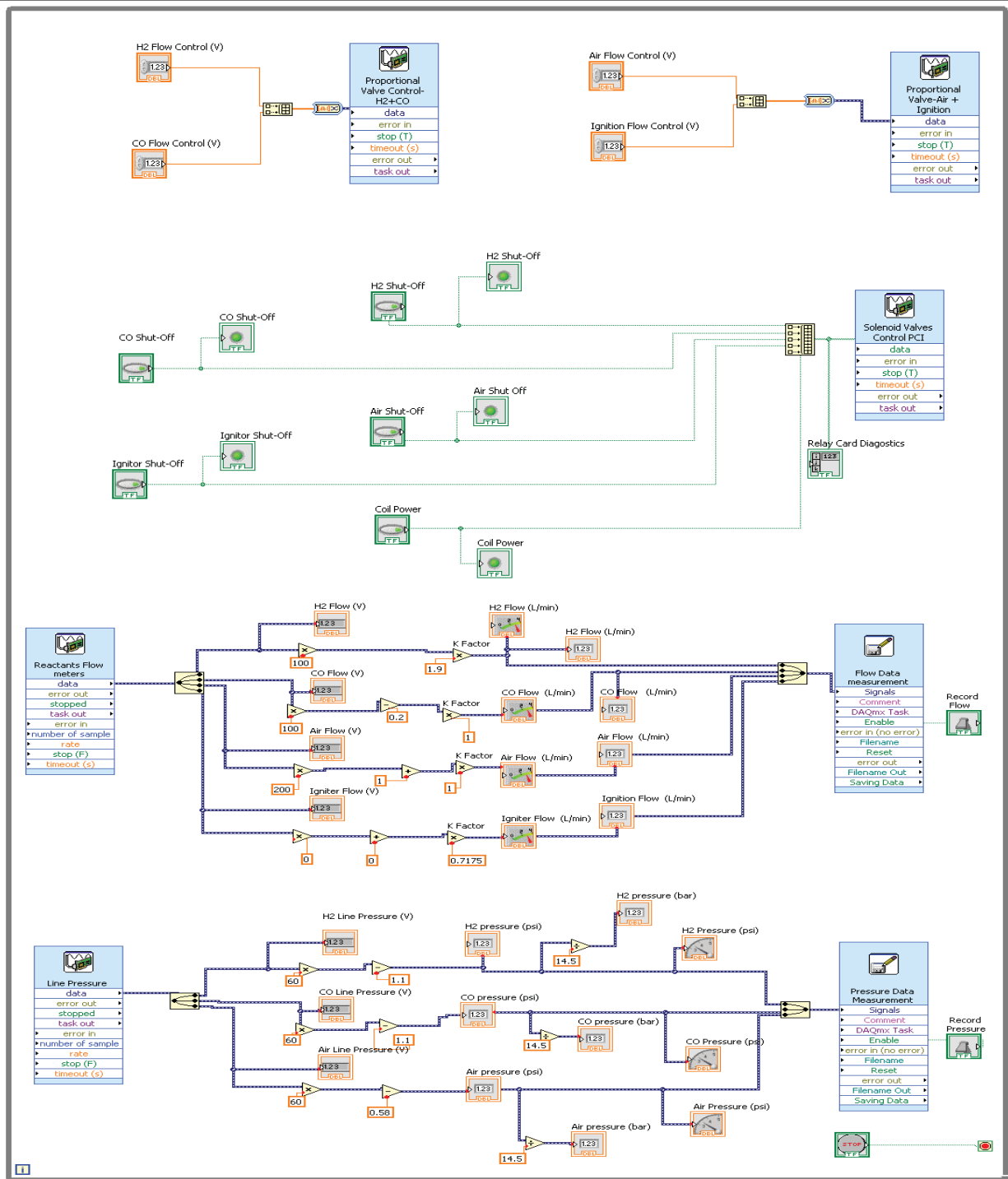
Figure 33 - Lab View block diagram configured for the high-pressure combustion system

High-pressure combustion system summary

The high pressure combustion system at the cSETR laboratory in the University of Texas at El Paso was designed and developed to test high hydrogen concentration fuels and study their stability as well as flames characteristics. The high-pressure combustor is capable of operating at pressures up to 1.5 MPa and a maximum temperature of 2400 K according to its adiabatic flame calculations. The combustor is controlled remotely via a Lab View Interface that controls 4 proportional valves, 4 solenoid valves, an ignition coil and it receives feedback from 4 flow meters in the hydrogen, carbon monoxide, air and methane respectively. Figure 34 shows the overall set-up of the high-pressure combustion system. Figure 35 illustrates a cut-off view of the high-pressure combustor inlet manifold, the combustion chamber, and variable exhaust throat.
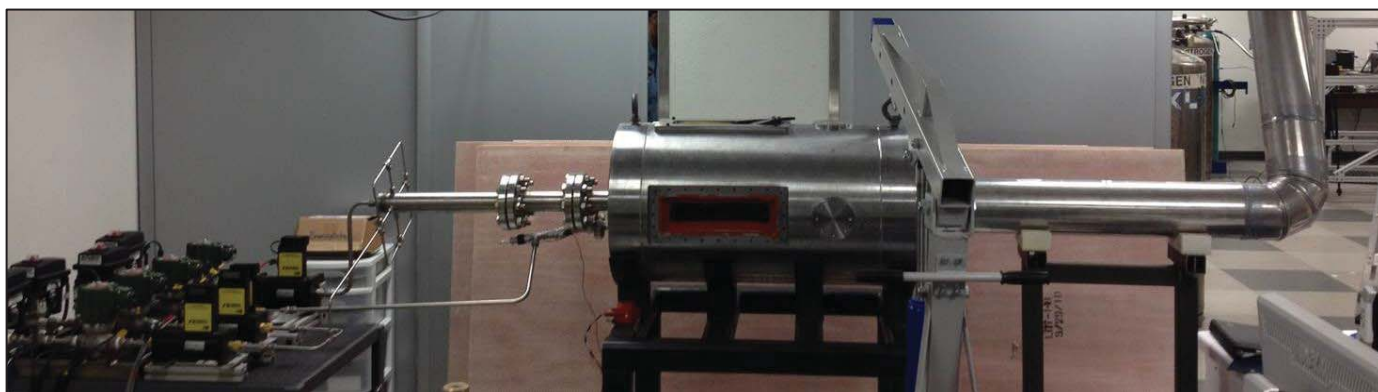
Figure 34 - High-pressure combustor: control system (left), combustion chamber (right)
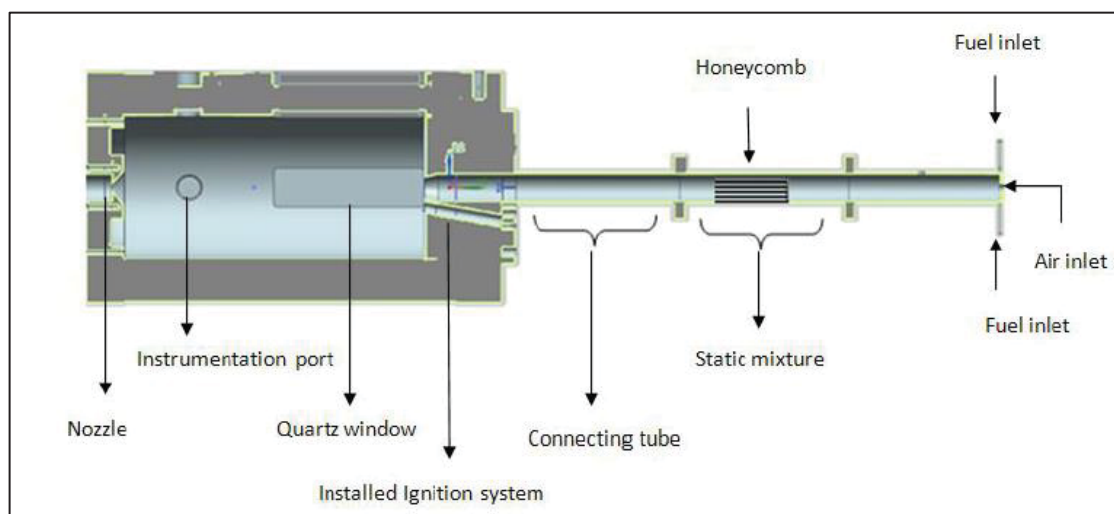
Figure 35 - high-pressure combustor cut-off view

40

3.2 Multi-Tube Injector (MTI) Gen-1

The MTI designed and developed to operate with high-hydrogen concentration fuel gases, to increase the stability of syngas flames, and to reduce pollutant emissions when compared with a swirl burner. The objective of the multi-tube fuel injector is to reduce flashback propensity and achieve stable flames a high-hydrogen content gas mixtures. The first generation of the MTI was designed with thirteen 4 mm orifices evenly distributed along the injector face. The size of the orifices was determined based in the hydrogen-quenching diameter. The MTI consist of 3 different parts: (i) Injector head, (ii) Connecting tube, and (iii) Base. All components in the MTI are made out of Stainless Steel 410 to maintain material uniformity among the entire high-pressure combustor system. Figure 36 illustrates the overall MTI used in the high-pressure combustion system at the cSETR lab.
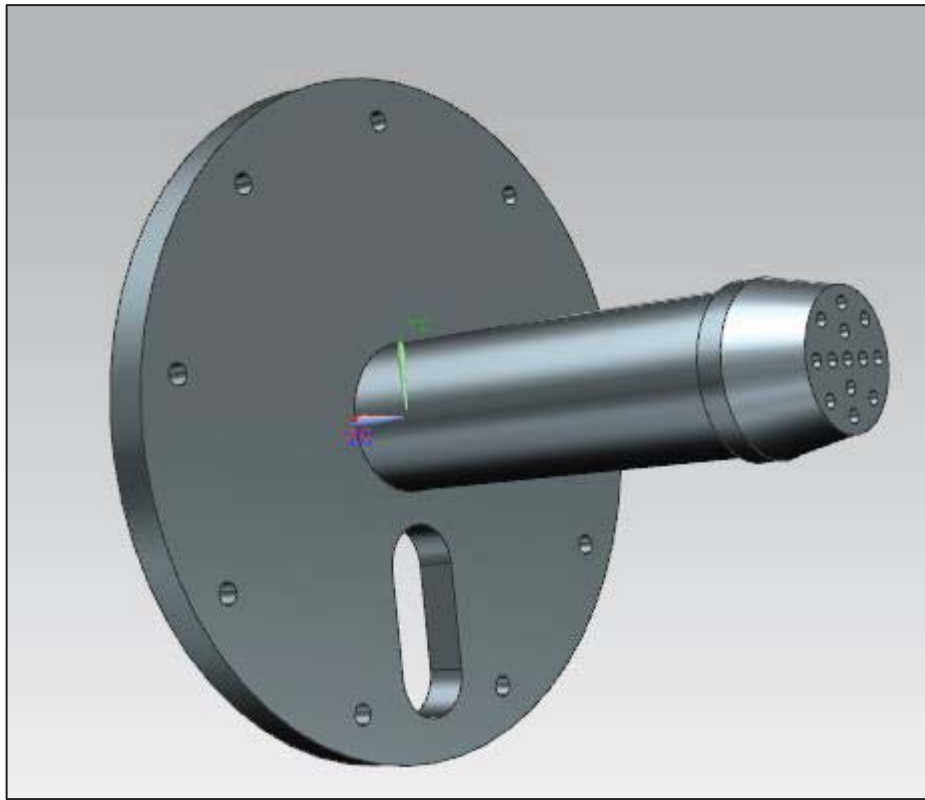
Figure 36 - Multi - Tube Fuel Injector for high-hydrogen fuels

3.2.1 Injector Head

The injector head consist in a stainless steel tube converged from a diameter of 5 to 3 cm. This converging reduction was done so the injector head can feel in the high-pressure combustor front cap. The injector head tube has 13 orifices of 0.004 m diameter and depths of 0.002 m. the orifices are apart by 7 mm while the orifices in the outer layer at 10 mm apart. Figure 37 illustrates the geometry of the injector head. The injector head bottom face was manufactured with a grouping in order to fit the connecting tube adequately. The bottom injector face can be observed in figure 38.
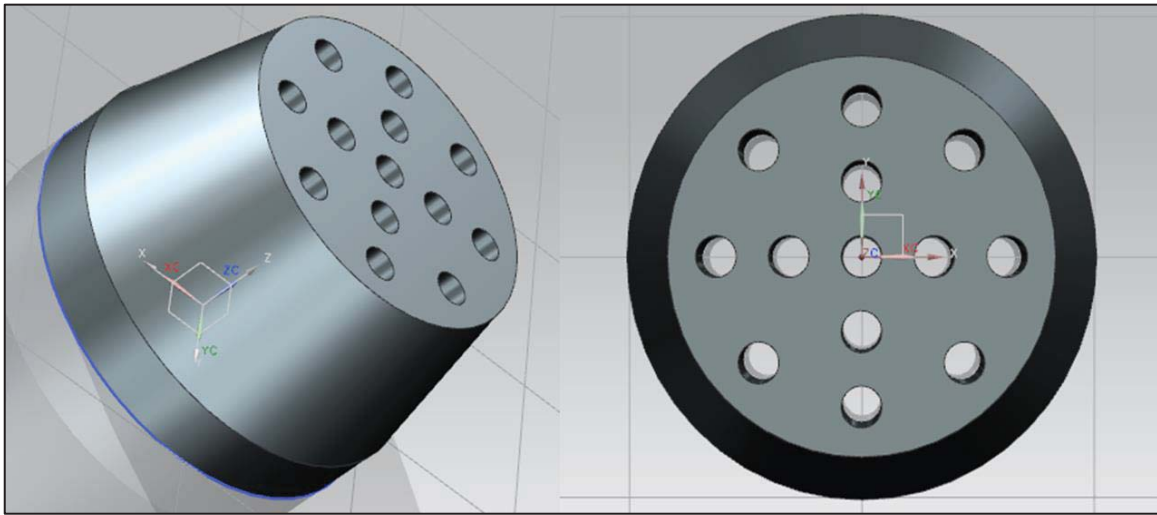
Figure 37 - MTI injector head geometry
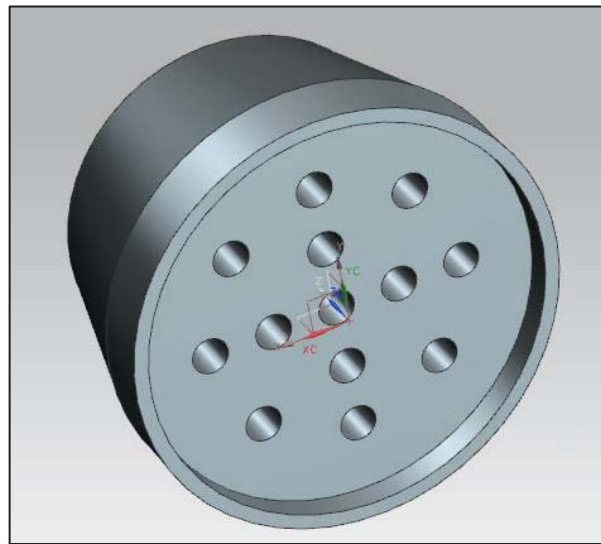
Figure 38 - Injector head bottom face

3.2.2   Connecting Tube

The connecting tube is assembled between the injector head and the base. The tube has a diameter of 3 cm and a height if 10 cm. Figure 39 illustrates the connecting tube portion of the MTI.
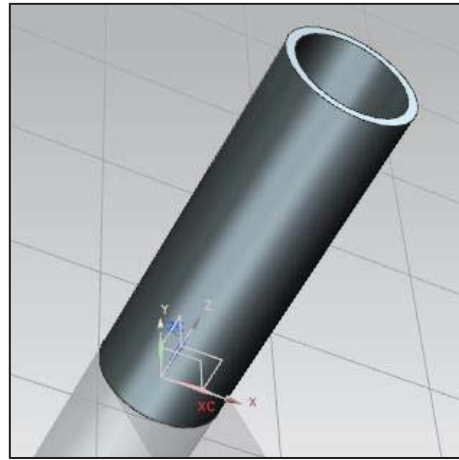
Figure 39 - MTI connecting tube

3.2.3   Base

The base is assembled with the connecting tube and it is connected to the front cap of the high-pressure combustor. The Base of the MTI is connected between the inlet manifold and the combustor front cap. The base has a diameter of 20 cm, it has nine 6 mm holes that serve to connect the injector the combustor front cap, and it has one 25 mm port to provide clearance for the ignition system when is connected to the combustion chamber. Figure 40 illustrates the MTI base.
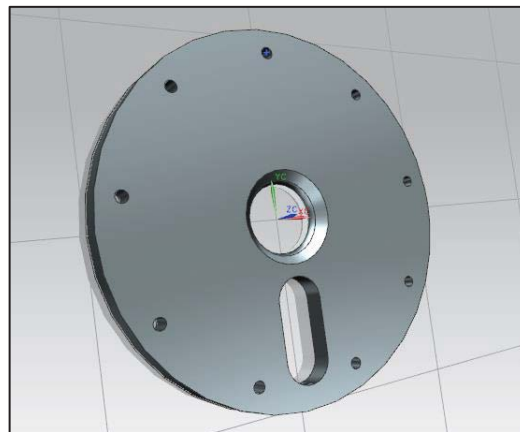
Figure 40 - MTI Base

3.3   Test Methodology

The objective of the tests performed in the high-pressure combustor system is to create a stability map by performing various experiments with high-content hydrogen fuels at various fuel compositions. The stability map will serve as a reference tool to identify the operation range at which any given fuel composition of syngas combusts with stability.

This paper present the results of testing syngas combustion at 20%, 30% and 40% hydrogen concentrations for lean conditions ranging from equivalence ratios of 0.6, 0.7, 0.8 and 0.9. The tests were performed using the Multi-Tube Fuel Injector (MTI) described in the previous sections. Each equivalence ratio (ϕ) of each fuel concentration was tested for various velocity ratios (v_r) of bulk velocity (v_{bulk}) over flame speed (s_L) ranging from 3 to 13.

3.3.1   Test Matrix

In order to carry out the tests it was necessary to determine various parameters such as flame speed (s_L) for each equivalence ratio, the hydrogen concentration in the syngas mixture, the density of the mixture of H₂-CO and air (ρ_{mix}) at any given condition, the actual air to fuel ratio($(A/F)_{actual}$), the mole fractions (x_i), and mass fractions (w_i) among others. Given that all this parameters are satisfied, it is possible to calculate which flow rate in liters per minute (LPM) is necessary to reach such conditions.

Flame speed

Flame speed was calculated in two different ways: (i) CHEMKIN kinetic code, using the GRI 2.0 mechanism, and (ii) by using flame speed based in literature and previous experiments.

CHEMKIN was used to calculate the flame speed of the fuel-air mixtures mentioned above. Figure 41 illustrates the results of flame speed at various fuel concentrations ranging from 10% to 90% hydrogen concentration in syngas-air mixtures.

44
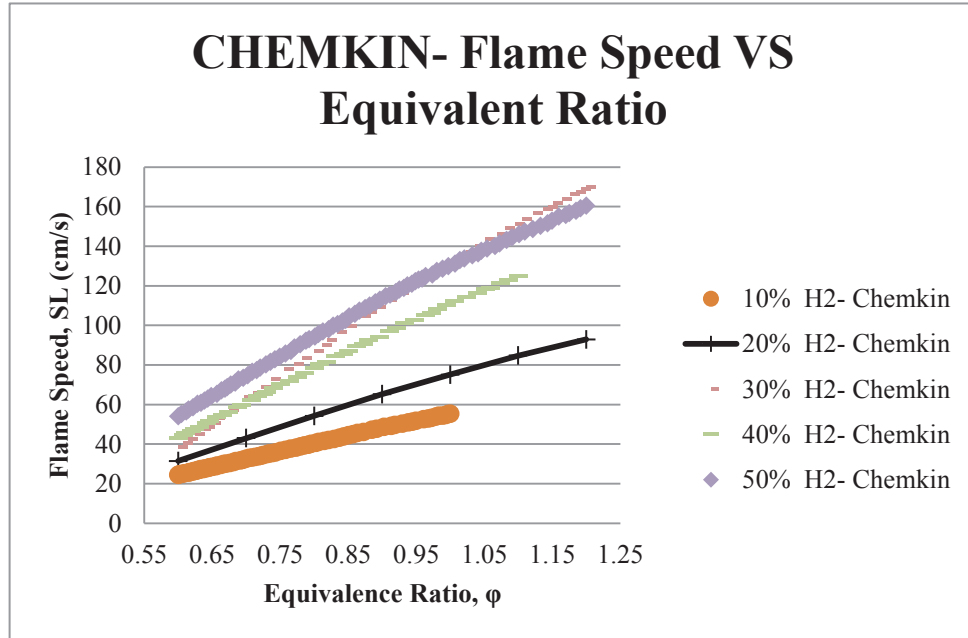
Figure 41 - CHEMKIN flame speed values for 10 to 90% hydrogen concentrations.

Figure 42 illustrates the flame speed (s_L) graph obtained from literature. The following flame speed were obtained as a function of equivalence ratio for various H_2/CO mixtures at P= 1atm and T_{in}= 330 K [6].
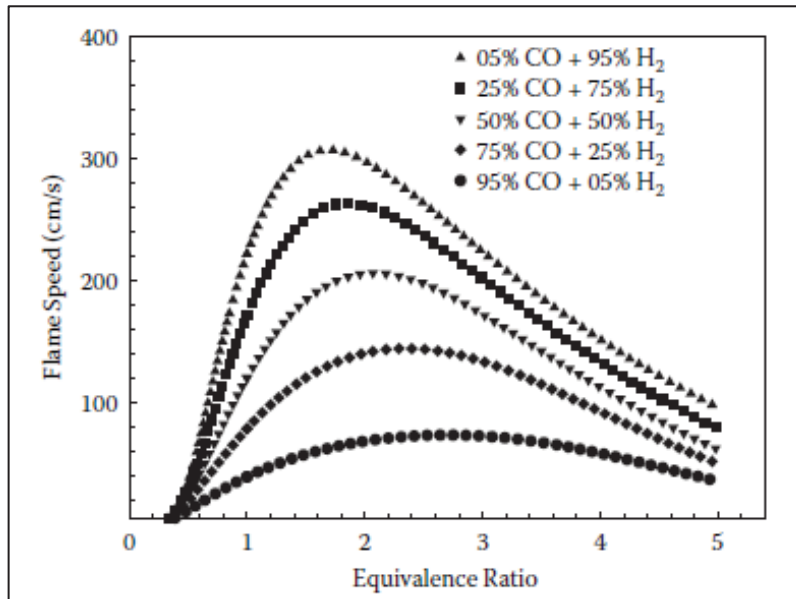
Figure 42 - Literature flame speed values at P= 1 atm and T-initial=300 K [6]

45

CHEMKIN flame speed values show a discrepancy in the 30% hydrogen content in syngas as it can be observed in Figure 41. Thirty percent hydrogen concentration indicates a greater flame speed than 40% and 50% above a 0.6 equivalence ratio. Literature flame speed values were chosen to perform the calculations in the test matrix since these values are more consistent in their estimation of flame speed.

Table 2 illustrates the flame speed values used for the experiments performed at the high-pressure combustor.

Table 2 - Literature flame speed values [6]

φ	20% H_2 - 80% CO SL (cm/s)	30% H_2 - 70% CO SL (cm/s)	40% H_2 - 60% CO SL (cm/s)
	LITERATURE FLAME SPEED		
0.6	21.39	26.10	31.80
0.7	33.30	42.07	51.76
0.8	44.42	56.95	70.28
0.9	54.70	70.59	87.09

Governing Equations

The following main equations were used in the test matrix to determine the quantity of H_2/CO and air necessary to achieve a specific syngas composition and equivalence ratio. Appendix C has a detailed breakdown of the test matrix governing equations. From equation 2 is possible to obtain the total fuel mass flow ($\dot{m}_{fuel}$).

$$\dot{m}_{fuel} = \frac{\rho_{mix} \cdot A_h \cdot n \cdot v_{bulk}}{\left(1 + \left(\frac{A}{F}\right)_{actual}\right)} \qquad (2)$$

Where ρ_{mix} is the density of the fuel-air mixture at any specific given mixture, A_h is the area of a single hole in the fuel injector, n are the number of holes in the injector, and v_{bulk} is the velocity of the fuel-air that the flowmeter read after its converted from LPM to m/s.

46

Once the mass flow of the fuel is obtained, equation 3 can be used to determine the air mass flow rate ($\dot{m}_{air}$).

$$\dot{m}_{air} = \left(\frac{A}{F}\right)_{actual} \dot{m}_{fuel} \quad (3)$$

Once the fuel and the mass flow rate have been found, the mass fraction corresponding to each fuel composition are used in order to determine the H_2 and CO mass flow rate. Table 3 shows the detail mass fractions for both hydrogen and carbon monoxide respectively.

Table 3 - Mass fractions for H_2 and CO

MASS FRACTIONS FOR H_2 AND CO		
% H_2 - % CO	W_{H_2}	W_{CO}
20% H_2 - 80% CO	0.018	0.982
30% H_2 - 70% CO	0.030	0.970
40% H_2 - 60% CO	0.045	0.955

The stoichiometric air to fuel ratio and the mix density for each fuel composition is illustrated in Table 3. Note that actual air to fuel ratio can be obtained by solving Eq. (4).

$$\varphi = \frac{\left(\frac{A}{F}\right)_{stoic}}{\left(\frac{A}{F}\right)_{actual}} \quad (4)$$

Table 4 - Stoichiometric air to fuel ratio and mix density

$(A/F)_{stoic}$ and ρ_{mix}		
% H₂ - % CO	ρ_{mix}	$(A/F)_{stoic}$
20% H₂ - 80% CO	1.121	3.01
30% H₂ - 70% CO	1.089	3.40
40% H₂ - 60% CO	1.058	3.90

3.4   Critical Stability Radius Ratio, r_{ST}

The critical stability radius ratio (r_{ST}) is defined as the ratio between the radius at which a stable flame is achieved (r_{SL}) over the radius of the burner hole (r_o). The velocity at the point r_{SL} is equal to the flame speed (s_L). The critical stability radius can be expressed with Eq. (5) for a single orifice.

$$r_{ST} = \frac{r_{SL}}{r_o} = \sqrt{1 - \left(\frac{U_{r_{SL}}}{2v_{avg,h}}\right)} \qquad (5)$$

Where $U_{r_{SL}}$ is equals to the flame speed of any given syngas fuel-air mixture, and $v_{avg,h}$ is the average velocity at the hole.

The critical stability radius ratio can be used as a design tool that will assist in finding the ideal conditions at which a stable flame can be achieved without experiencing flashback or blowout conditions. This variable r_{ST} is an experimental constant obtained as result of testing syngas-air combustion at 20%, 30% and 40% hydrogen concentration in the fuel mixture.

Considering the MTI described in section 3.2 illustrated in Figure 43 where v_{bulk} is the velocity at which the gas enters the injector connecting tube after is passes through the inlet manifold. The velocity detected by the flow meters will be equal to v_{bulk}, R_o is the radius of the connecting tube, R_h is the distance from the center of the connecting tube to the center to the furthest hole from the center in the injector head, and $U_{(R_h)}$ is the local velocity of the gas at the distance R_h.
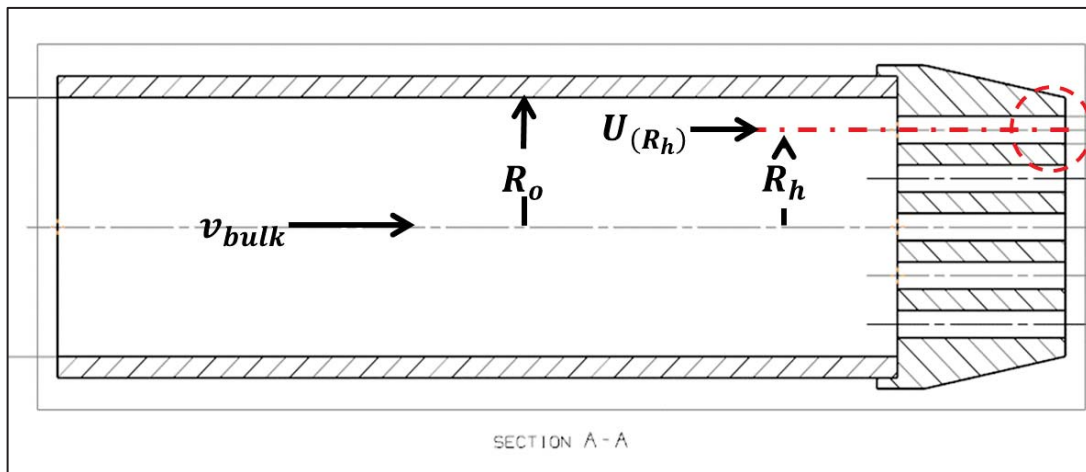
Figure 43 - Multi-tube fuel injector section view

Consider the red circle in the right top corner of Fig. 43. A section view of this orifice is illustrated in Fig. 44 below.
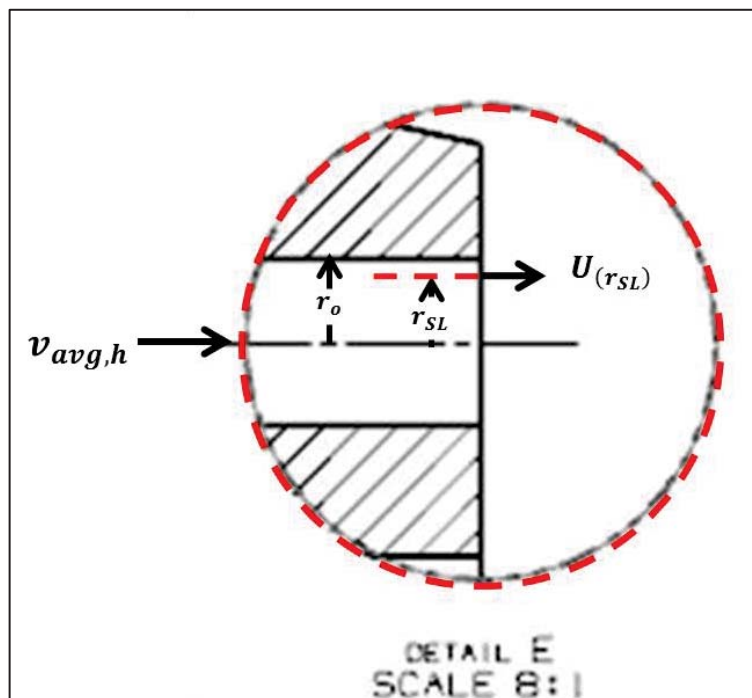
Figure 44 - Section of top upper hole in the injector head.

In Fig. 44 r_o is the radius of the hole in the injector head and $U_{(r_{SL})}$ is the local velocity when equal to the flame speed, r_{SL} is the distance from the center of hole in the injector head at which the

49

velocity is equals to the flame speed, and $v_{avg,h}$ is the average velocity in the hole at the injector head which is equals to $U_{(R_h)}$.

Given that r_{SL} can be found experimentally, it is possible to calculate the critical stability radius ratio. The variable r_{ST} can be graphed as a function of equivalence ratio. Figure 45 illustrates an example of a critical stability radius ratio as a function of equivalence ratio graph. This graph will establish a stability region within a specific syngas fuel mixture. Any value below the stability region indicates a propensity to flashback and any value above the stability region is in a blowout condition.
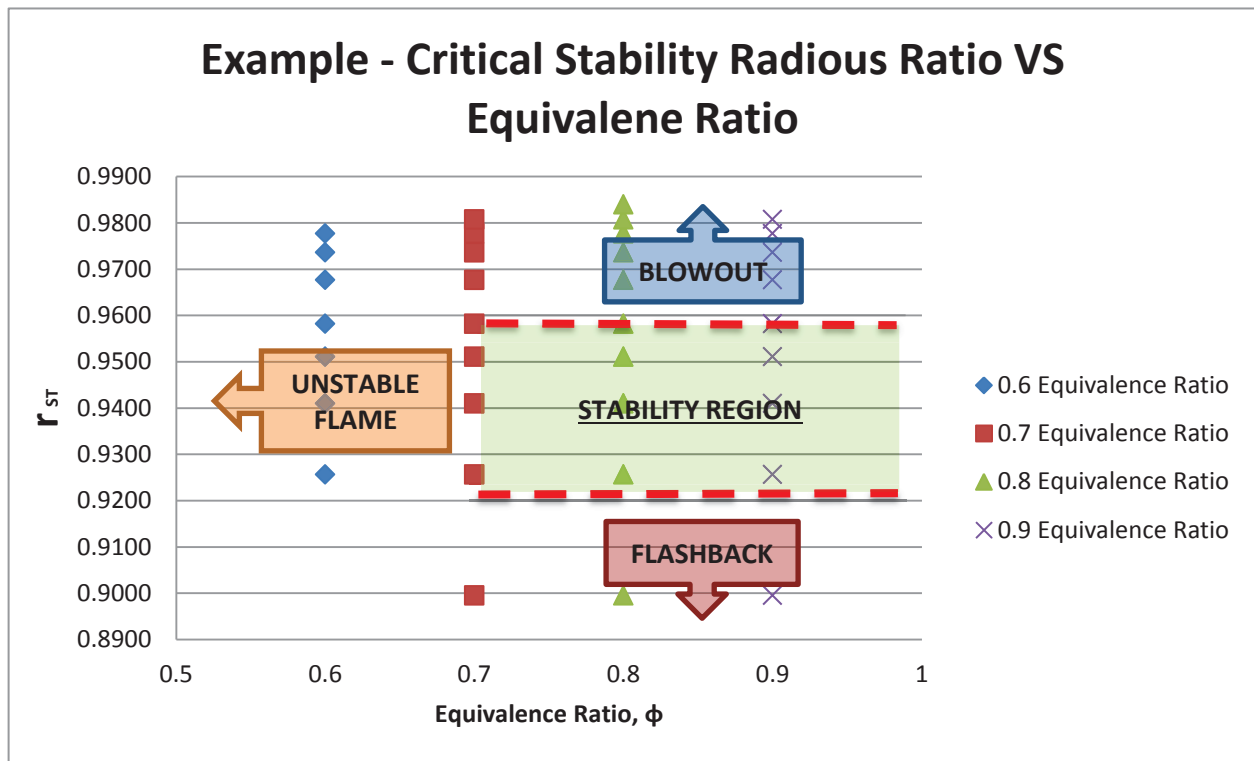
Figure 45 - Critical Stability Ratio as a function of Equivalence Ratio

The critical stability radius ratio can be used as a design tool to find specific conditions such as inlet bulk velocity for stability. Bulk velocity can then be input into Eq. (2) where the fuel mass flow can be obtained and subsequently air flow rate also. Equation 6 uses the critical stability radius ratio to determine the bulk velocity necessary to sustain a stable flame in the multi-tube flame injector.

$$v_{bulk} = \frac{U_{r_{SL}}}{4(1-r_{ST}^2)\left(1-\left(\frac{R_h}{R_o}\right)^2\right)} \quad (6)$$

The main purpose of the critical stability radius ratio is to find the exact distance r_{SL} at which is possible to obtain a stable flame. As the velocity distribution along the orifice radius r_o changes it is important to find at which distance flashback propensity occurs, when a stable flame is achieved, and when flame blow out occurs. The critical stability radius ratio is a dimensionless number that can assist in finding operational windows for any given fuel mixture as well as specific injector design.

Laminar velocity distribution along the orifice diameter was assumed in order to perform these calculations. This laminar velocity distribution is assumed to simplify and perform calculations with a dependence on radius and average velocity. Given that the velocity close to the wall of the pipe is low due to the non-slip condition, it is useful to use the laminar velocity distribution since the area of interest in the calculation is the one close to the wall and not the in the center of the pipe or orifice.

In order to be able to use the critical stability radius ratio it is important that the following requirements are met:

1. The equations are only valid for syngas fuel mixtures of 20, 30 and 40% hydrogen concentrations
2. The injector geometry must be a single level face; the holes must be in the same plane.
3. All holes in the injector face must be of the same diameter, $D = 4\,mm$
4. All calculations must be performed for the furthest hole from the center of the injector. The furthest hole from the center of the injector is located at a distance R_h and it experiences the lowest velocity given its proximity to the pipe wall.

Chapter 4: Results & Conclusions

Chapter 4 will discuss the results obtained of testing syngas – air combustion at 20, 30 and 40% hydrogen concentrations at equivalence ratios φ=0.6, 0.7, 0.8, and 0.9. This chapter will illustrate the testing points used during such experiments and will present the stability maps and critical stability radius ratio maps. The stability maps are illustrated as the bulk velocity as s function of equivalence ratio. The critical stability radius ratio maps are illustrated as a function of equivalence ratio.

4.1   Test Uncertainty

Knowing the testing uncertainty is important because it gives a level of confidence and repeatability to our results. Uncertainty is present throughout all the devices that record specific information that can potentially have an error margin. The high-pressure combustor system flowmeters are the only measurement system utilized this are the only value that can be subjected to measurement errors. Measurements range of error was calculated for the critical flowmeters which are H_2, CO and Air flowmeters respectively. Relative error was calculated for φ=0.7, 30% H_2 - 70% CO. Table 5, 6 and 7 illustrate the results and potential error margin in the experimentation process.

Table 5 - Relative error of H_2 flow meter

H_2 Flow Meter Relative Error		
H_2 Flow – Expected Value (LPM)	H_2 Flow – Actual Value – Average (LPM)	Relative Error %
1.11	1.12	0.8
1.39	1.40	0.8
1.67	1.66	-0.4
1.95	1.90	-2.3
2.50	2.50	0.0

Table 6 - Relative error of CO flow meter

CO Flow Meter Relative Error		
CO Flow – Expected Value (LPM)	CO Flow – Actual Value – Average (LPM)	Relative Error %
2.60	2.15	-17.3
3.25	3.35	3.1
3.90	3.96	1.5
4.55	4.60	1.1
5.85	5.74	-1.9

Table 7 - Relative error of Air flow meter

Air Flow Meter Relative Error		
Air Flow – Expected Value (LPM)	Air Flow – Actual Value – Average (LPM)	Relative Error %
12.42	12.10	-2.5
15.52	15.37	-1.0
18.62	18.42	-1.1
21.73	21.50	-1.1
27.94	28.40	1.7

Given the results presented in Tables 5, 6 and 7, the experimental results obtained from our tests will have a high degree of confidence since the error margin is within +3%, -2.5%. Therefore we can say that the results are repeatable within an acceptable limit.

4.2 Test Results

4.2.1 20% H₂ - 80% CO

Tables 8 through 11 show the specific points tested for this fuel-air mixture.

Table 8 - 0.6 equivalence ratio 20% H_2 - 80% CO

20 % H₂ - 80% CO		Φ=0.6	$S_L = 0.214\ m/s$
v_{bulk}/S_L	H₂ Flow (LPM)	CO Flow (LPM)	Air Flow (LPM)
4.0	0.33	1.34	6.53
5.0	0.42	1.68	8.17
6.0	0.50	2.01	9.80
7.0	0.58	2.35	11.43
9.0	0.75	3.02	14.70
11.0	0.92	3.69	17.97
13.0	1.09	4.36	21.23

Table 9 - 0.7 equivalence ratio 20% H_2 - 80% CO

20 % H₂ - 80% CO		Φ=0.7	$S_L = 0.333\ m/s$
v_{bulk}/S_L	H₂ Flow (LPM)	CO Flow (LPM)	Air Flow (LPM)
4	0.59	2.37	9.89
5	0.74	2.96	12.37
6	0.89	3.55	14.84
7	1.03	4.14	17.31
9	1.33	5.33	22.26
11	1.62	6.51	27.21
13	1.92	7.70	32.15
15	2.21	8.88	37.1

54

Table 10 - 0.8 equivalence ratio 20% H$_2$ - 80% CO

20 % H$_2$ - 80% CO		Φ=0.8	$S_L = 0.444\ m/s$
v_{bulk}/S_L	H$_2$ Flow (LPM)	CO Flow (LPM)	Air Flow (LPM)
3.0	0.66	2.64	9.64
4.0	0.88	3.52	12.85
5.0	1.10	4.39	16.07
6.0	1.31	5.27	19.28
7.0	1.53	6.15	22.49
9.0	1.97	7.91	28.92
11.0	2.41	9.67	35.34
13.0	2.85	11.42	41.77

Table 11 - 0.9 equivalence ratio 20% H$_2$ - 80% CO

20 % H$_2$ - 80% CO		Φ=0.9	$S_L = 0.547\ m/s$
v_{bulk}/S_L	H$_2$ Flow (LPM)	CO Flow (LPM)	Air Flow (LPM)
4	1.18	4.75	15.42
5	1.48	5.93	19.28
6	1.77	7.12	23.13
7	2.07	8.30	26.99
9	2.66	10.68	34.70
11	3.25	13.05	42.41
13	3.85	15.42	50.12

Figure 46 illustrates the stability map for syngas with hydrogen concentration on 20%. The combustion produced from this fuel mixture showed a small stability range with some stability observed at a 0.6 equivalence ratio, Fig. 48. Stability increased as equivalence ratio increased. Stable points were found at 0.7 equivalence ratio, however the stability area resulted to be very small as with bulk velocity increase produced a lifted flame with blowout tendencies as it can be illustrated in Figs. 49 to 51. Despite the small stability area, the multi tube injector demonstrated to have an even greater stable lifted region in which bulk velocity needed to be increased greatly before flame blowout. The critical stability ratios region, illustrated in Fig. 47, is relatively low for 20% hydrogen concentration in the fuel mixture.
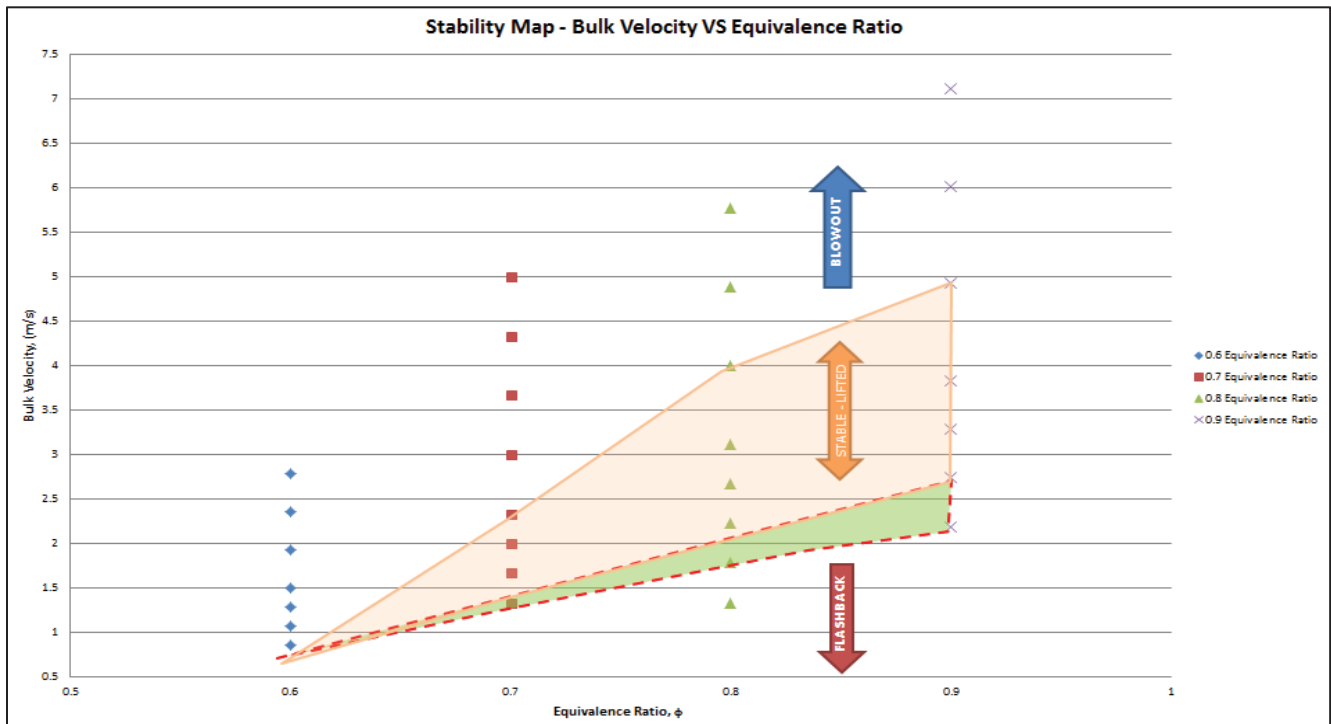
Figure 46 – Stability map bulk velocity as a function of equivalence ratio 20% H_2 Concentration

Figure 47 - Critical Stability Radius Ratio as a function of equivalence ratio, 20% H_2 concentration

56

Figure 48 - 20% H$_2$, ɸ=0.6, Vbulk/SL = 4, 5 and 9

Figure 49 - 20% H$_2$, φ=0.7, Vbulk/SL = 5, 6 and 13

Figure 50 - 20% H$_2$, φ=0.8, Vbulk/SL = 4, 6 and 11

Figure 51 - 20% H$_2$, φ=0.9, Vbulk/SL = 3, 6 and 11

57

4.2.3 30% H₂ - 70% CO

Tables 12through 15 show the specific points tested for this fuel-air mixture.

Table 12 - 0.6 equivalence ratio 30% H$_2$ - 70% CO

30 % H₂ - 70% CO		Φ=0.6	$S_L = 0.261\ m/s$
v_{bulk}/S_L	H₂ Flow (LPM)	CO Flow (LPM)	Air Flow (LPM)
4	0.61	1.42	7.90
5	0.76	1.77	9.87
6	0.91	2.13	11.84
7	1.06	2.48	13.82
9	1.36	3.19	17.76
11	1.67	3.90	21.71
13	1.97	4.61	25.66

Table 13 - 0.7 equivalence ratio 30% H$_2$ - 70% CO

30 % H₂ - 70% CO		Φ=0.7	$S_L = 0.421 m/s$
v_{bulk}/S_L	H₂ Flow (LPM)	CO Flow (LPM)	Air Flow (LPM)
3	0.83	1.95	9.31
4	1.11	2.60	12.42
5	1.39	3.25	15.52
6	1.67	3.90	18.62
7	1.95	4.55	21.73
9	2.50	5.85	27.94
11	3.06	7.15	34.14
13	3.61	8.45	40.35
15	4.17	9.75	46.56

The 30% hydrogen concentration in the syngas fuel mixture increased the stability region compared with 20% concentration in the mixture, Fig. 52. Just as the 20% hydrogen concentration in the fuel mixture, the 0.6 equivalence ratio did not provide a stable flame. The flames illustrated in Fig. 54 are examples of 30% hydrogen concentrations at a 0.6 equivalence ratio. These flames are unstable with a tendency towards flame blowout. Combustion of syngas at a 30-70 H$_2$-CO provided positive results for the critical stability radius ratio graph in which there is a constant stability region between points 0.926 to 0.950.

Table 14 - 0.8 equivalence ratio 30% H_2 - 70% CO

30 % H_2 - 70% CO		Φ=0.8	$S_L = 0.569\ m/s$
v_{bulk}/S_L	H_2 Flow (LPM)	CO Flow (LPM)	Air Flow (LPM)
3	1.26	2.95	12.31
4	1.68	3.93	16.41
5	2.10	4.91	20.51
6	2.52	5.89	24.61
7	2.94	6.87	28.71
9	3.78	8.84	36.92
11	4.62	10.80	45.12
13	5.46	12.76	53.33
15	6.29	14.73	61.53
18	7.55	17.67	73.84

Table 15 - 0.9 equivalence ratio 30% H_2 - 70% CO

30 % H_2 - 70% CO		Φ=0.9	$S_L = 0.706\ m/s$
v_{bulk}/S_L	H_2 Flow (LPM)	CO Flow (LPM)	Air Flow (LPM)
3	1.71	4.01	14.90
4	2.29	5.35	19.87
5	2.86	6.69	24.83
6	3.43	8.02	29.80
7	4.00	9.36	34.77
9	5.14	12.04	44.70
11	6.29	14.71	54.63
13	7.43	17.38	64.57
15	8.57	20.06	74.50

Figure 53 shows the ideal Critical Stability Radius Ratio region that can be utilized for design and flame stability uses. Although the critical stability radius ratio regions illustrated in Figs. 47 and 48 can be used, the stability region in Fig. 53 does provide standard measure for more than one equivalence ratio.

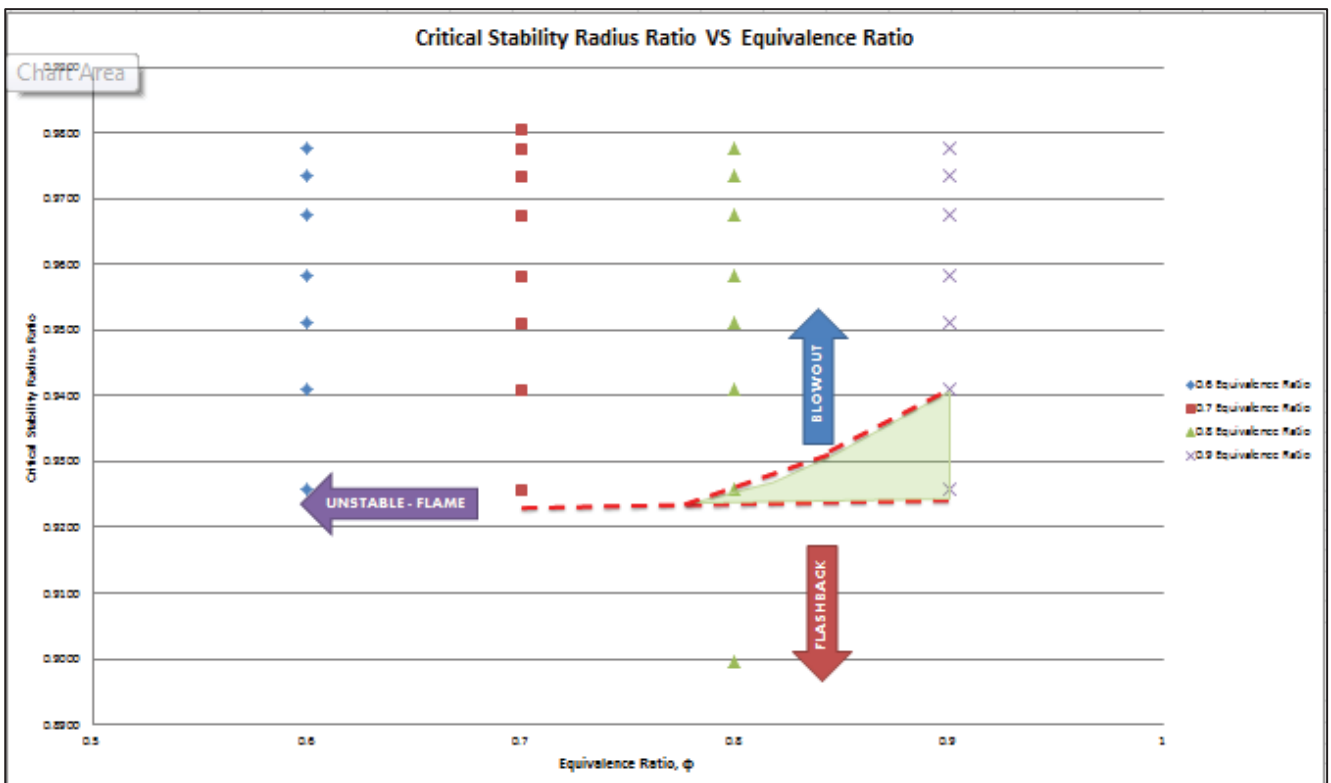Figure 52 - Stability map bulk velocity as a function of equivalence ratio 30% H_2 Concentration

Figure 53 - Critical Stability Radius Ratio as a function of equivalence ratio, 30% H_2 concentration
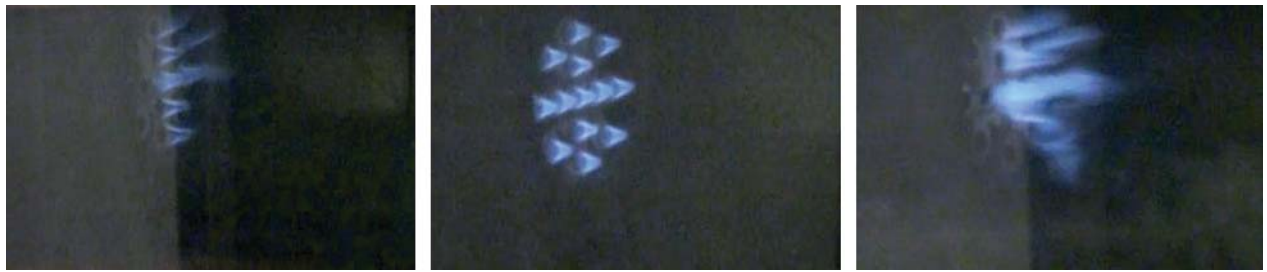
Figure 54 - 30% H$_2$, φ=0.6, Vbulk/SL = 3, 4 and 6
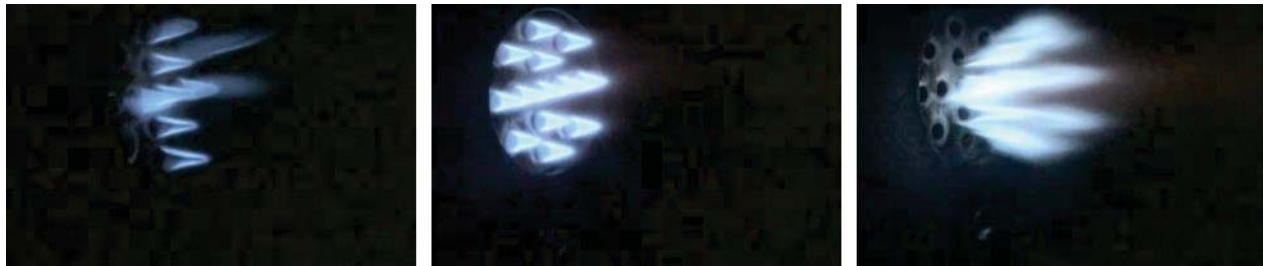
Figure 55 - 30% H$_2$, φ=0.7, Vbulk/SL = 3, 5 and 11
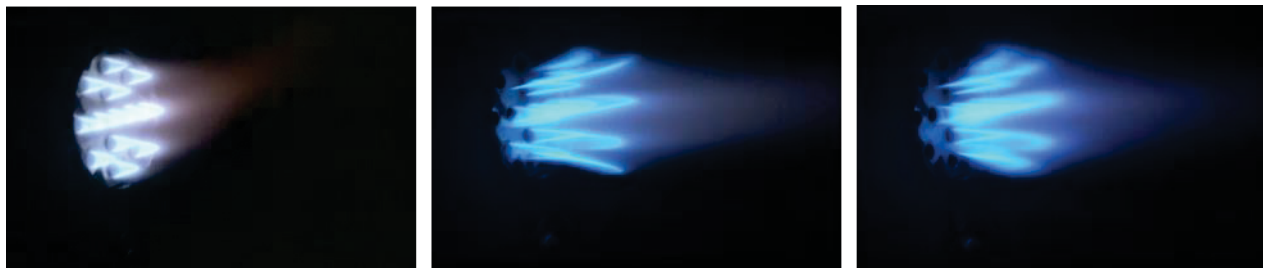
Figure 56 - 30% H$_2$, φ=0.8, Vbulk/SL = 4, 13 and 15

Figure 57 - 30% H$_2$, φ=0.9, Vbulk/SL = 3, 5 and 13

61

4.2.3 40% H₂ - 60% CO

Tables 16 through 19 show the specific points tested for this fuel-air mixture.

Table 16 - 0.6 equivalence ratio 40% H$_2$ - 60% CO

40 % H$_2$ - 60% CO		Φ=0.6	$S_L = 0.318\,m/s$
v_{bulk}/S_L	H$_2$ Flow (LPM)	CO Flow (LPM)	Air Flow (LPM)
4	0.97	1.47	9.53
5	1.22	1.83	11.91
6	1.46	2.20	14.29
7	1.71	2.57	16.67
9	2.19	3.30	21.44
11	2.68	4.03	26.20
13	3.17	4.76	30.96
15	3.65	5.50	35.73

Table 17 - 0.7 equivalence ratio 40% H$_2$ - 60% CO

40 % H$_2$ - 60% CO		Φ=0.7	$S_L = 0.518\,m/s$
v_{bulk}/S_L	H$_2$ Flow (LPM)	CO Flow (LPM)	Air Flow (LPM)
4	1.81	2.72	15.17
5	2.26	3.40	18.96
6	2.72	4.08	22.75
7	3.17	4.76	26.55
9	4.07	6.13	34.13
11	4.98	7.49	41.72
13	5.88	8.85	49.30

Table 18 - 0.8 equivalence ratio 40% H_2 - 60% CO

40 % H_2 - 60% CO		Φ=0.8	$S_L = 0.703\ m/s$
v_{bulk}/S_L	H_2 Flow (LPM)	CO Flow (LPM)	Air Flow (LPM)
4	2.75	4.14	20.16
5	3.44	5.17	25.20
6	4.12	6.20	30.24
7	4.81	7.24	35.28
9	6.19	9.30	45.36
11	7.56	11.37	55.44
13	8.94	13.44	65.51
15	10.31	15.51	75.59

Table 19 - 0.9 equivalence ratio 40% H_2 - 60% CO

40 % H_2 - 60% CO		Φ=0.9	$S_L = 0.871\ m/s$
v_{bulk}/S_L	H_2 Flow (LPM)	CO Flow (LPM)	Air Flow (LPM)
4	3.75	5.64	24.46
5	4.69	7.06	30.57
6	5.63	8.47	36.69
7	6.57	9.88	42.80
9	8.45	12.70	55.03
11	10.32	15.52	67.26
13	12.20	18.35	79.49

The use of a 40% hydrogen concentration in syngas fuel mixtures results in the greatest stability in syngas flames. It can be concluded that the multi-tube injector used for the experiments presented in this thesis operates better as hydrogen content increases in the syngas fuel mixture. Figure 59 illustrates the stability region of 40% hydrogen concentration under the green area. The stable lifted region is the greatest for the 40% fuel concentration. The flame produced by this syngas fuel mixture proved to be resistant to blowout requiring a very high velocity to reach a flame lift off, Fig. 63. The critical stability radius ratio region in Fig. 59 shows that the stability points increased with 40% hydrogen concentration. However, this region is not constant when compared with Fig. 53 at a 30% hydrogen concentration.
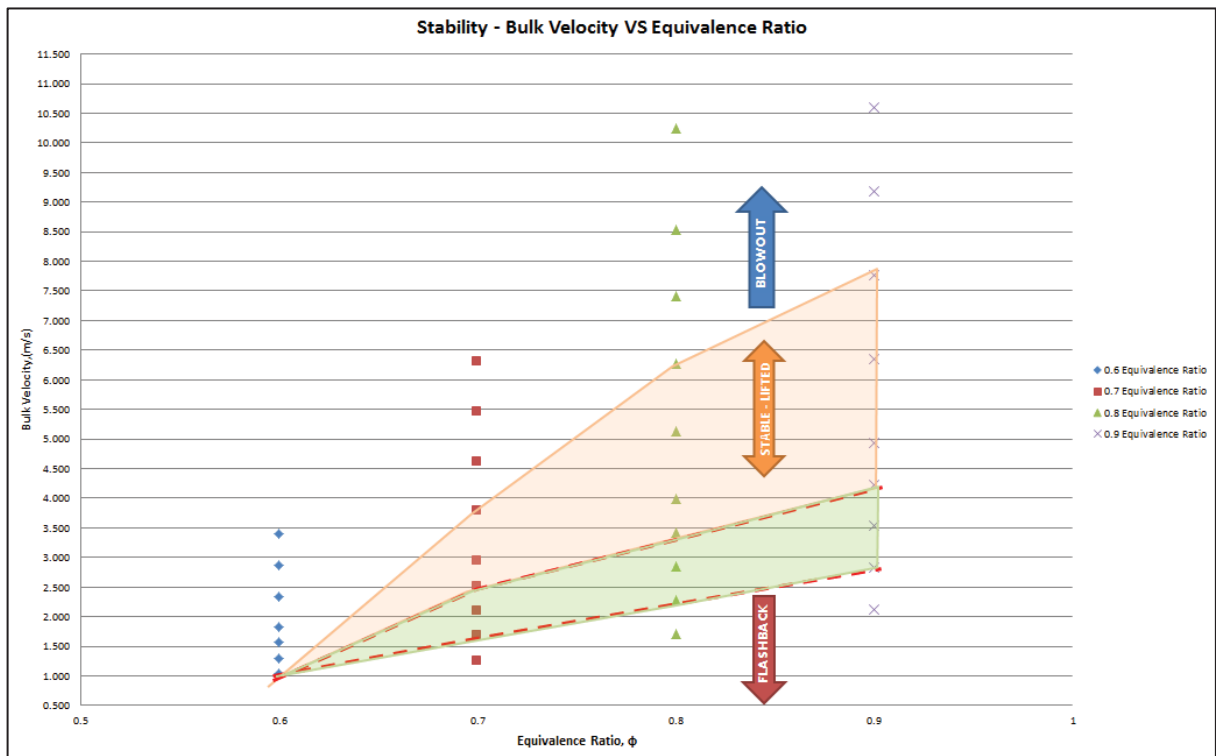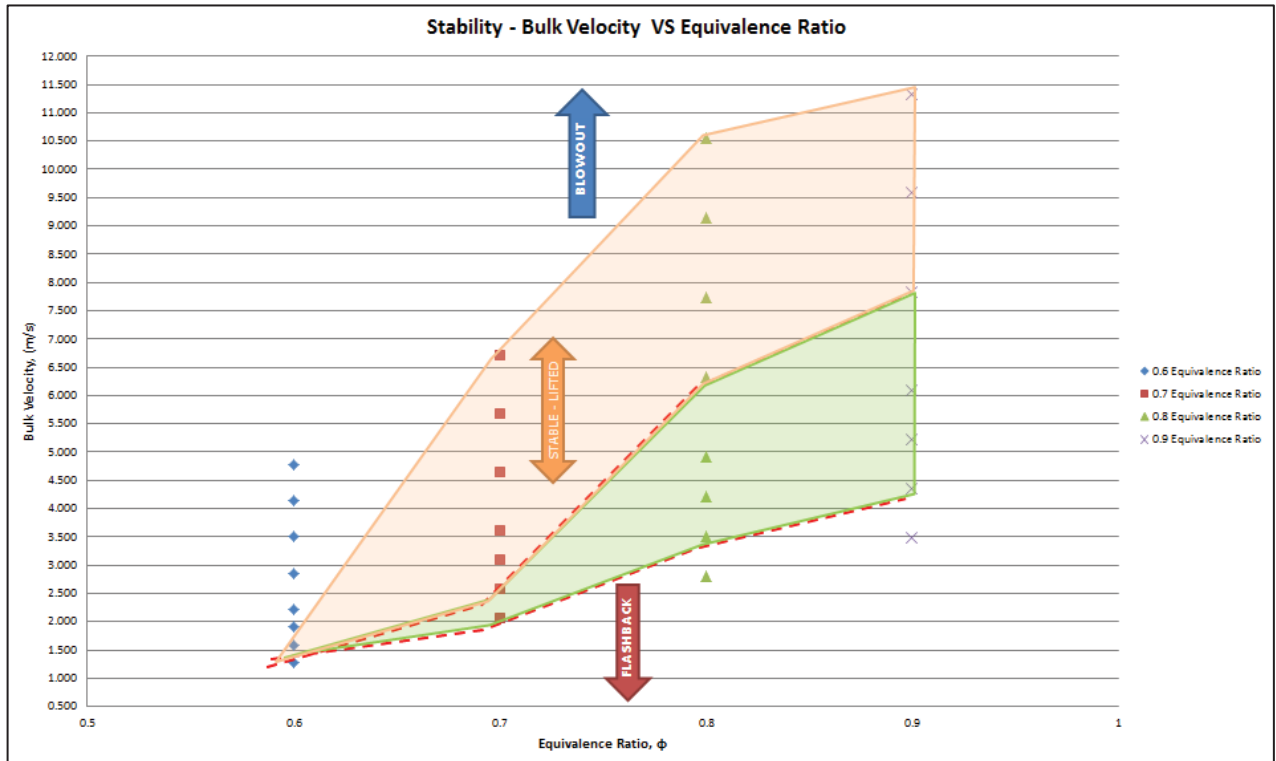
Figure 58 - Stability map bulk velocity as a function of equivalence ratio 40% H_2 Concentration
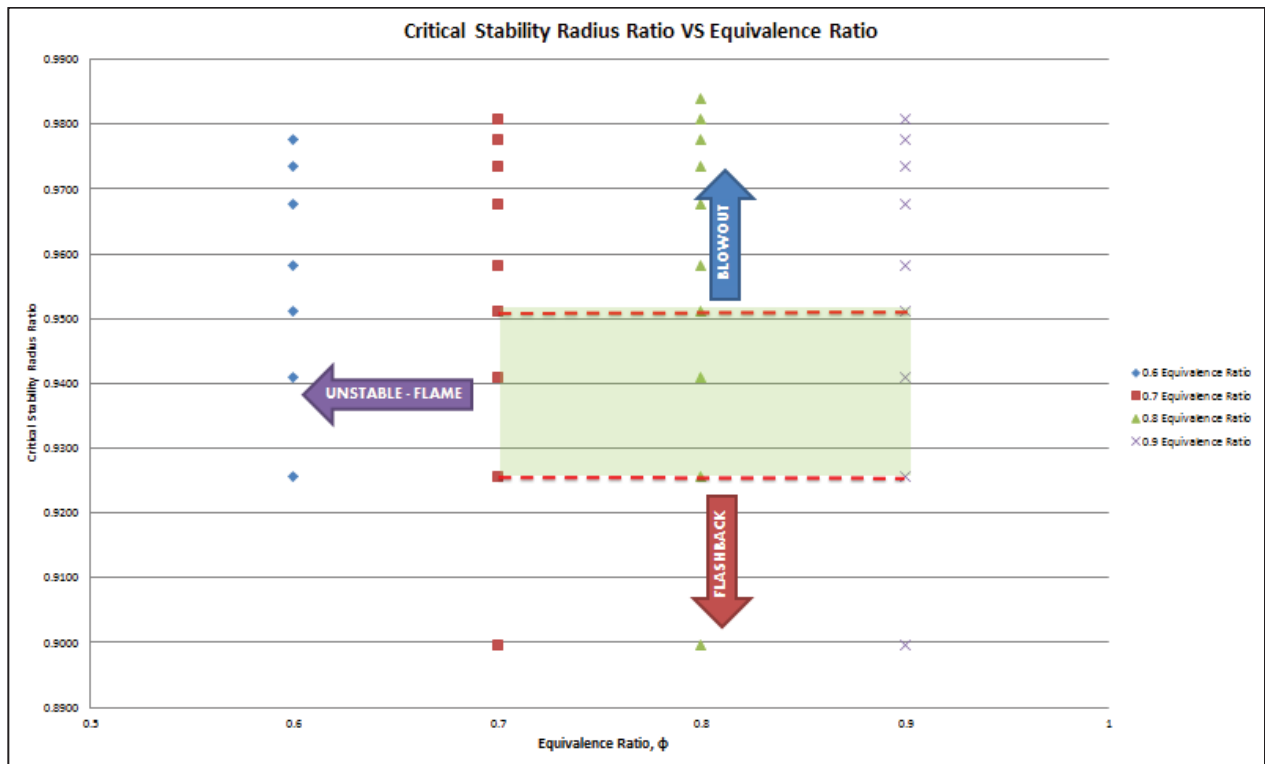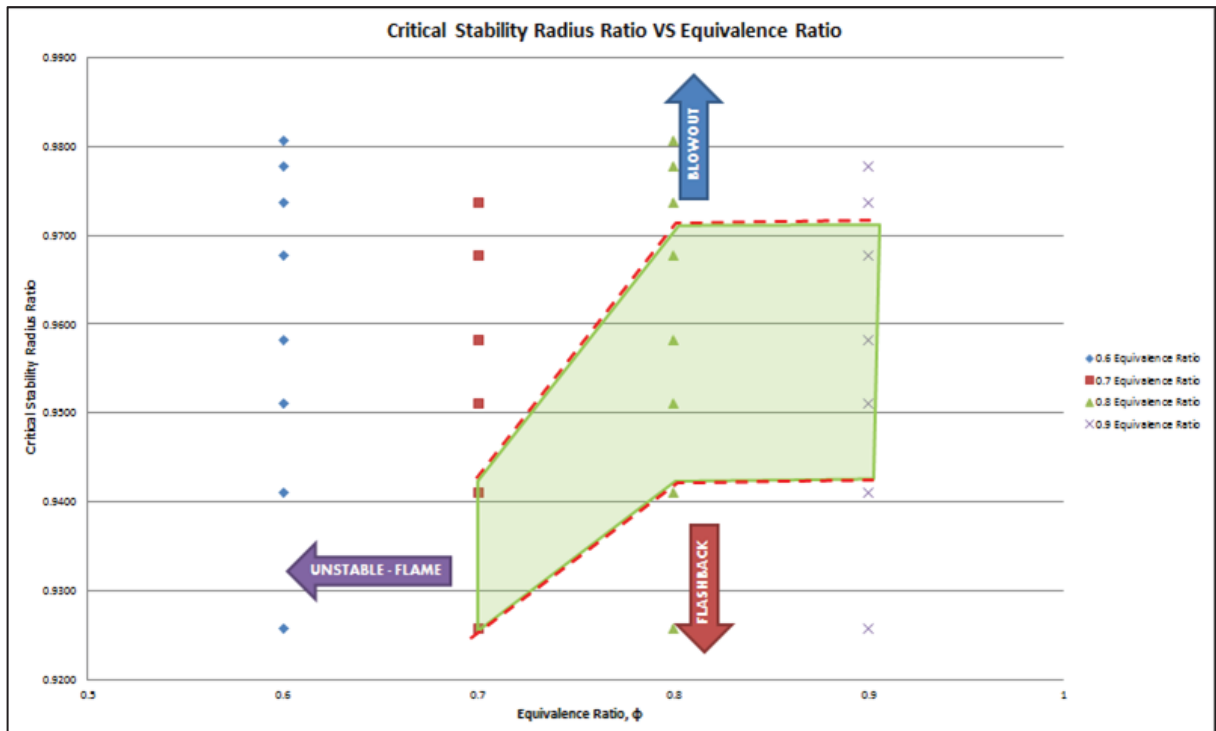

Figure 59 - Critical Stability Radius Ratio as a function of equivalence ratio, 40% H_2 concentration
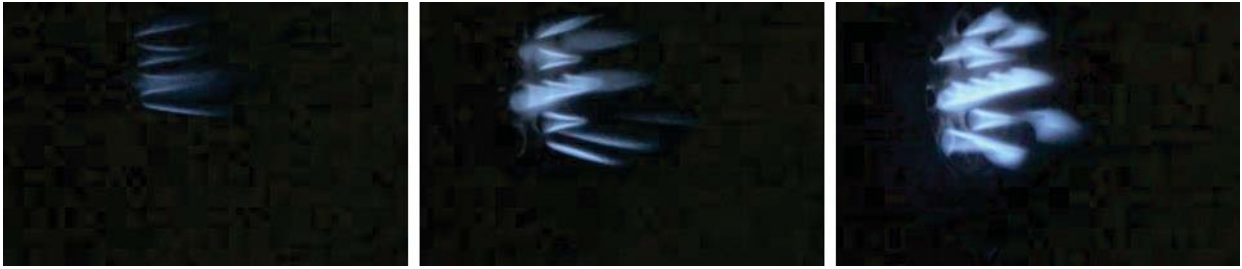
Figure 60 - 40% H_2, φ=0.6, Vbulk/SL = 4, 5 and 9

Figure 61 - 40% H_2, φ=0.7, Vbulk/SL = 4, 7 and 13

Figure 62 - 40% H_2, φ=0.8, Vbulk/SL = 4, 9 and 15

Figure 63 - 40% H_2, φ=0.9, Vbulk/SL = 4, 7 and 13
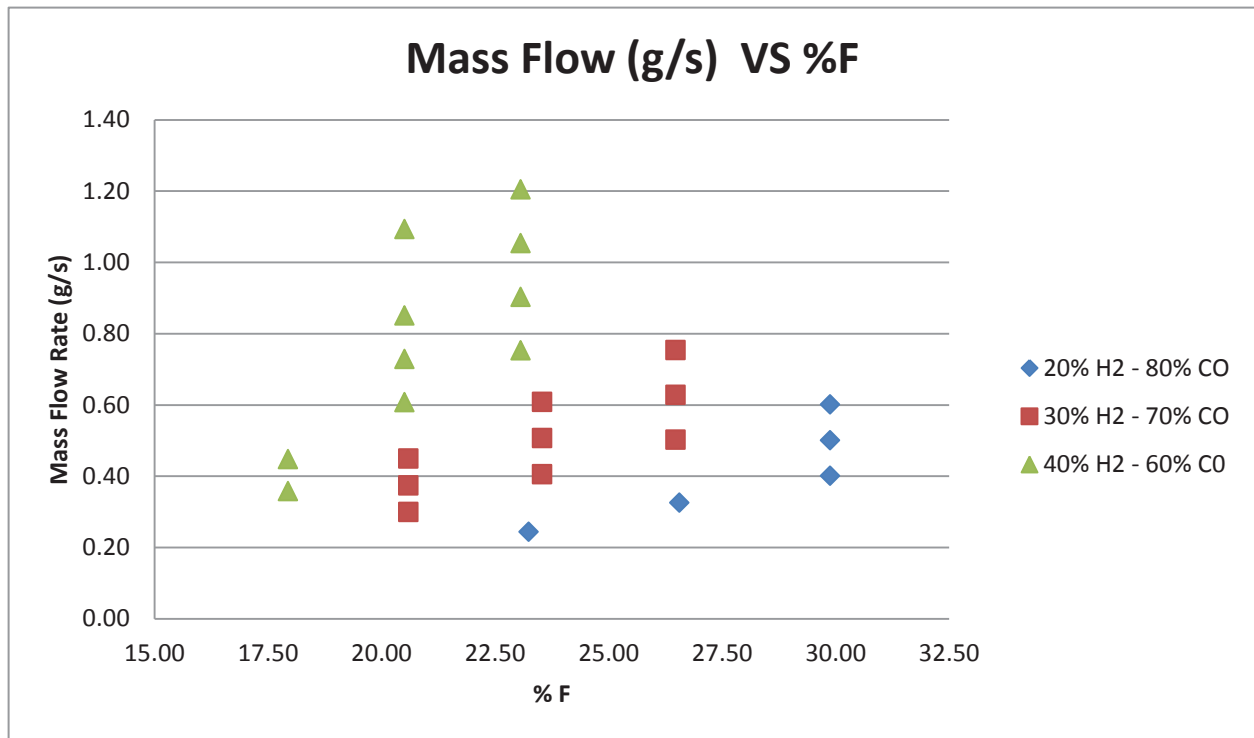
Figure 64 - Mass Flow VS percentage of fuel, % Fuel
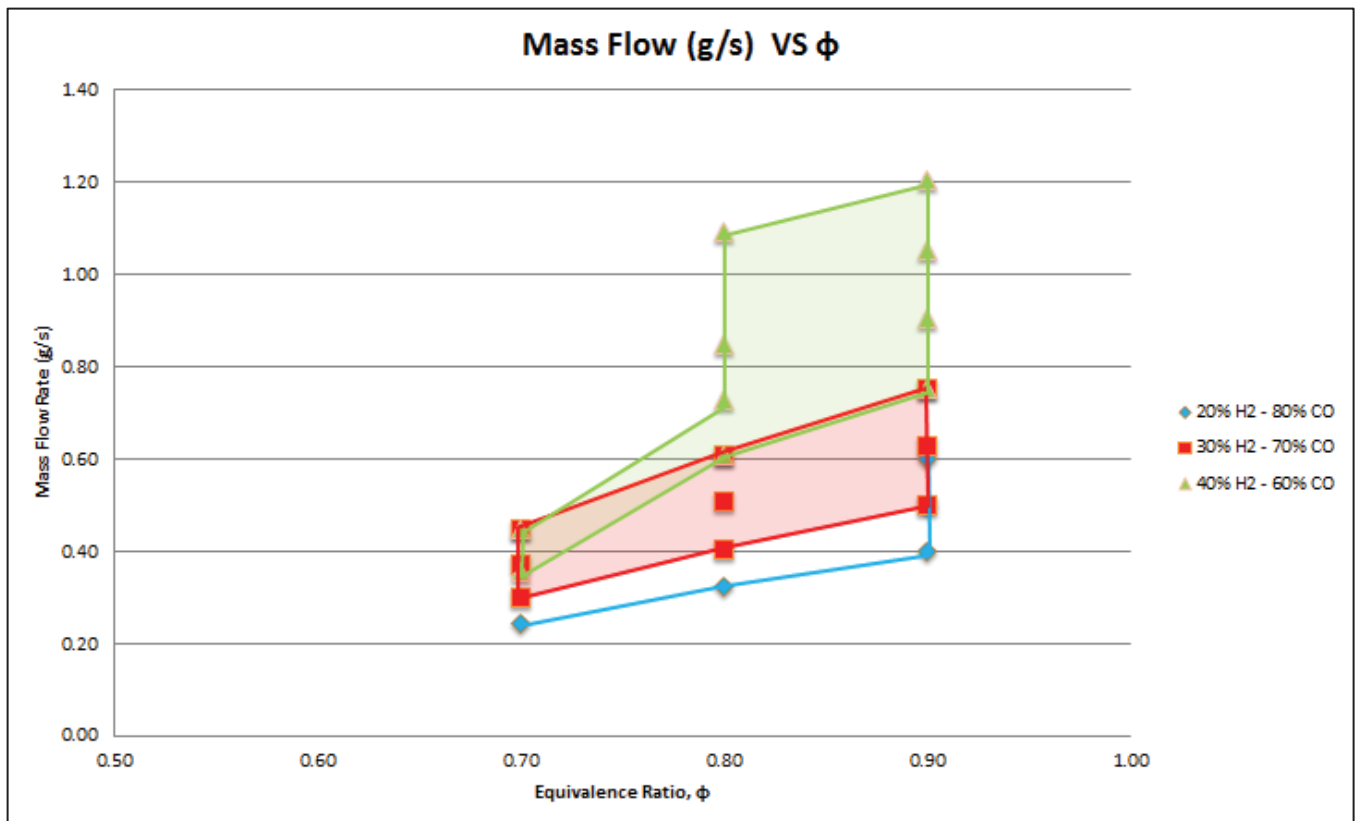
Figure 65 - Stability Regions - Mass Flow VS Equivalence Ratio

66
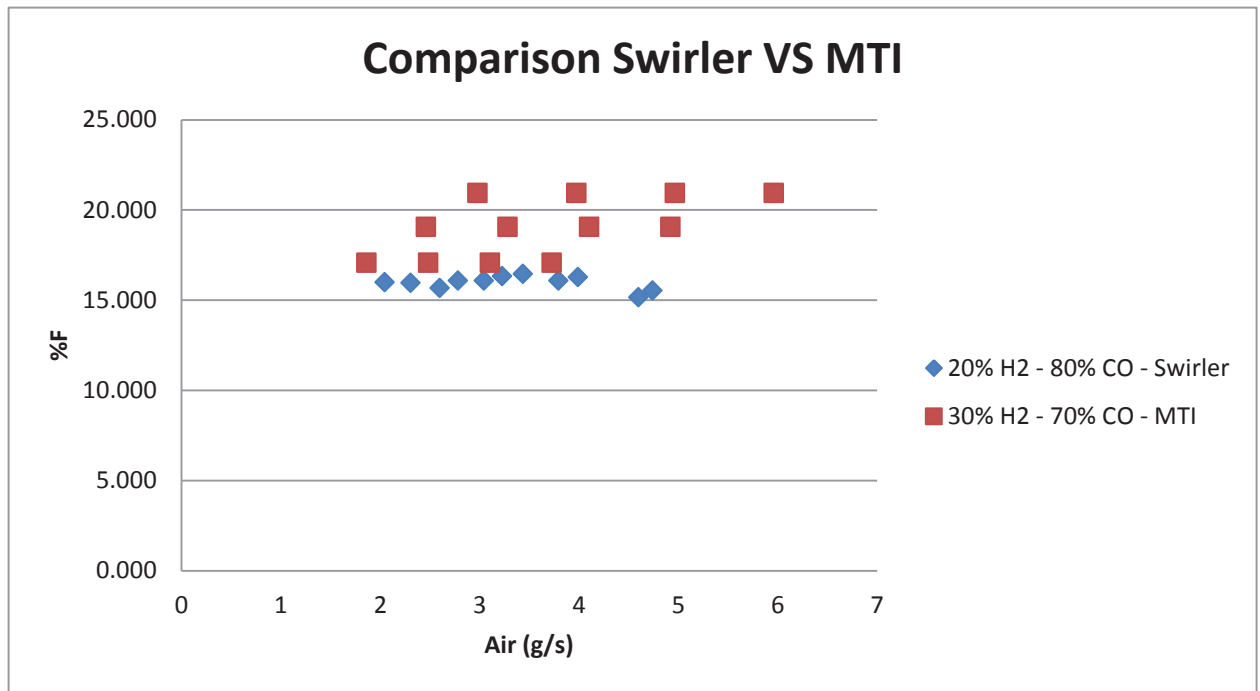
Figure 66 - Comparison of Swirler VS MTI stability
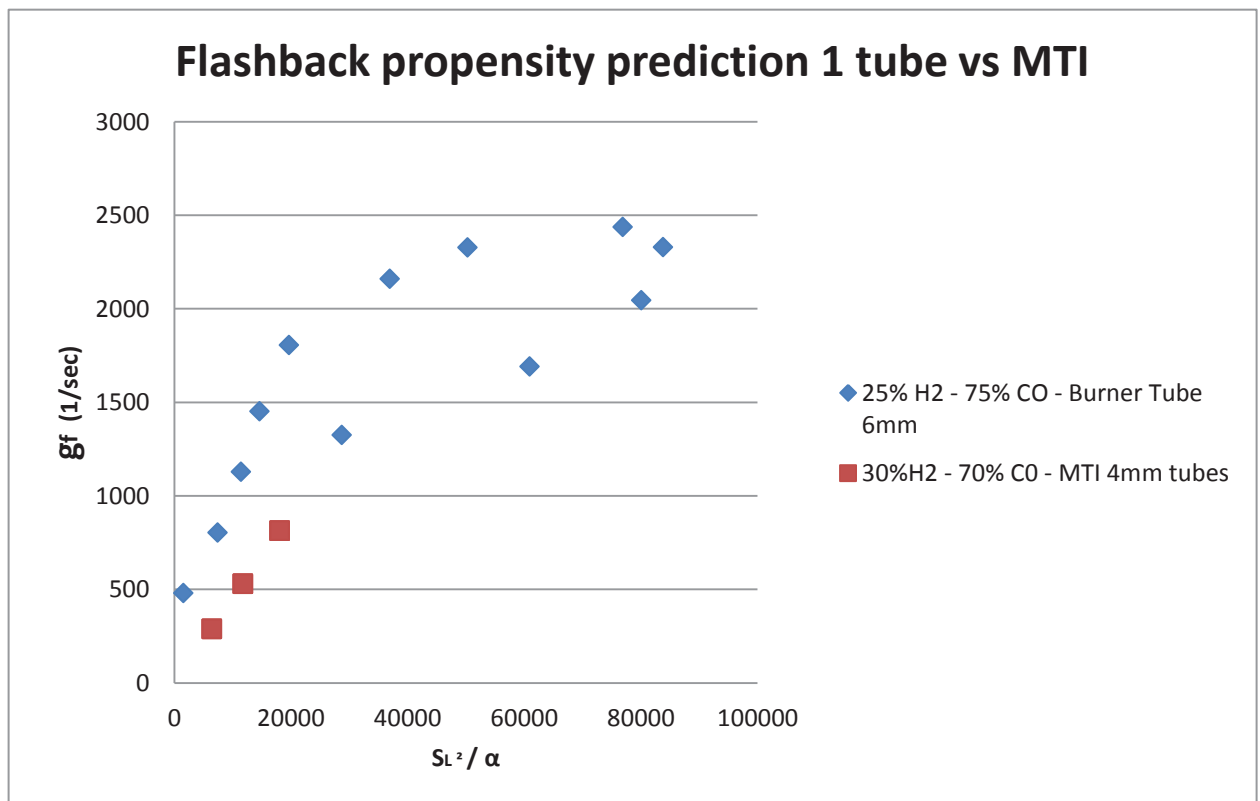
Figure 67 - Comparison of flashback propensity between 1 tube and MTI

Figure 64 and 64 illustrate a relationship of mass flow rate as a function of percentage of fuel and equivalence ratio respectively. It can be observed that as the percentage of hydrogen increases in the fuel mixture, the fuel concentration decreases as hydrogen is less dense as compared with carbon monoxide. Ideally, it is preferable to use the highest mass flow rate and the lowest fuel concentration in the mixture. By doing so, there is more mass output than can be translated in more energy being produced and also, there is less fuel being used.

Graphs 66 and 67 present a comparison of results obtained from the experimentation with the MTI and swirl injectors. Also, the MTI was compared with flashback predictions for a single 6mm tube.

4.3   Design Improvements

After extensive experimentation, it was determined that the outer injector ports have direct influence in flashback and blowout behaviors, hence all calculations for stability were performed for the outer injector ports. A strong stability interaction between the injector ports was observed after the testing. It was found that more stable flames can be appreciated in the areas of the injector with 5 aligned holes compared to the areas with 3 consecutive holes. Figure 68 illustrated both 5 continuous holes and 3 continuous holes arrangements in the injectors respectively.
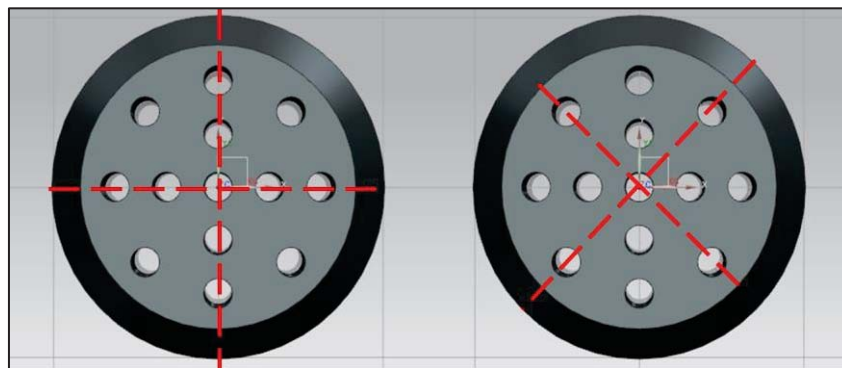
Figure 68 - five continuous holes arrangement (left) and three continuous holes arrangement (right)

It was observed that the outer holes located at 45°, 135°, 225°, and 315° experience the most instabilities when the combustor operates at stable-lifted conditions. This issue can be mitigated by adding holes and decreasing the distance between holes. Therefore, increasing injector ports will not only improve the injector's stability, but also it will increase firing output. Figure 69 illustrates two suggested designs of injector faces that will assist in increasing stability.
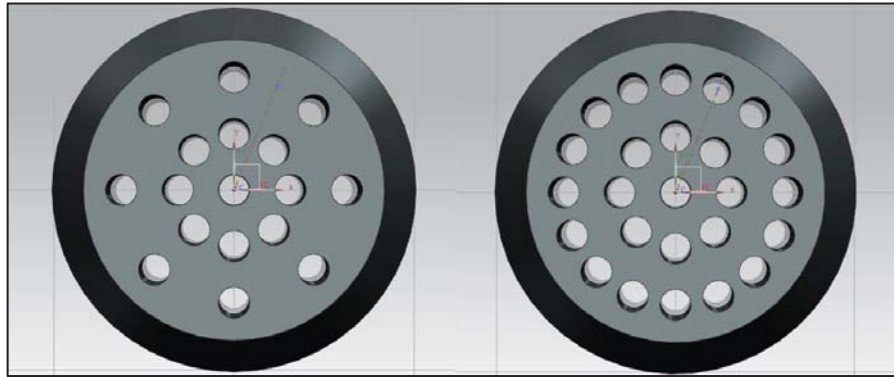
Figure 69 - New injector head design

Chapter 5: Summary and Future Work

The work in this thesis presents the experimental study of syngas combustion aimed to find stability of H_2/CO- air flames at 20, 30 and 40% hydrogen concentration in the fuel mixture using a multi-tube fuel injector. The experiments performed tested stability at lean conditions for equivalence ratios of 0.6, 0.7, 0.8 and 0.9. The experiments presented in this work were performed in the High Pressure Combustion facility in the Center for Space Exploration Technology Research (cSETR) Laboratory at the University of Texas at El Paso. The multi-tube fuel injector used to perform the stability experiments consisted of three 410 stainless steel parts: (i) injector head with thirteen 4mm orifices, (ii) a connecting tube, and (iii) a base which is connected to the front cap of the high-pressure combustor.

The experimental results showed that at an equivalence ratio of 0.6 it is not possible to obtain a stable flame for any of the fuel mixtures tested. It was also observed that the stability region of the syngas flame increases as the hydrogen concentration in syngas fuel increases. The 40% hydrogen-

carbon monoxide mixture demonstrated the greatest stability region. It was also found that there is a stable-lifted flame region above the stability region. The stable-lifted region was found to exist over a larger region than the stable flame region. The stable-lifted region increased as the hydrogen concentration in syngas fuel mixtures increased. High amounts of hydrogen in fuel mixtures allow the multi-tube to operate at higher velocities without flame blowout. Very high bulk velocities are required to blowout a syngas flame.

The critical stability radius ratio (r_{ST}) was also introduced and is defined as the ratio between the radius at which a stable flame is achieved (r_{SL}) over the radius of the burner hole (r_o). The velocity at the point r_{SL} is equal to the flame speed (s_L). The critical stability radius ratio can be used to find ideal stability operation parameter as well as a design tool. Experimental results showed that 30% hydrogen concentration in syngas produced an ideal critical stability radius ratio region between points 0.926 – 0.950 which can be used as a standard region for equivalence ratios of 0.7, 0.8 and 0.8.

It was found through experimentation that there is a strong interaction between the multi-tube injector burner holes. The vertical and horizontal holes in the multi-tube fuel injector demonstrated to be more stable compared to the 4 holes located at 45°, 135°, 225°, and 315° respectively. The future design of the multi-fuel injector must include an increase of burner holes evenly throughout its face to increase stability among the injector burner holes.

Additional experiments above a 40% hydrogen concentration must be performed to further understand the behavior of the multi-tube fuel injector with high hydrogen concentration in syngas fuel mixtures.

Works Cited

[1]   "What is the role of cole in the United States?," U.S. Energy Information Administration, february 2014. [Online]. Available: http://www.eia.gov/energy_in_brief/article/role_coal_us.cfm.

[2]   "Energy.gov," [Online]. Available: http://energy.gov/fe/how-gas-turbine-power-plants-work. [Accessed 26 March 2014].

[3]   Energy and Enviromental Analysis (and ICF International Company), *Technology Characterization: Steam Turbines,* Arlington, 2008.

[4]   S. R. Turns, An Introduction to Combustion, 2nd ed., McGraw-Hill , 2000.

[5]   J. P. Valentine, "EPA Proposes Carbon Pollution Standards for New Power Plants / Agency takes important step to reduce carbon pollution from power plants as part of President Obama's Climate Action Plan," United States Environmental Protection Agency, [Online]. Available: http://yosemite.epa.gov/opa/admpress.nsf/0/da9640577ceacd9f85257beb006cb2b6!OpenDocument. [Accessed 1 March 2014].

[6]   T. Lieuwen, V. Yang and R. Yetter, Eds., Synthesis Gas Combustion: Fundamental and Applications, CRC Press, 2010.

[7]   B. Dam, N. Love and C. Ahsan, "Flashback propensity of syngas fuels," *elsevier,* pp. 618-625, 2010.

[8]   Department of Energy, "National Energy Technology Laboratory," [Online]. Available: http://www.netl.doe.gov/technologies/coalpower/turbines/. [Accessed 6 june 2007].

[9]   R. Narula, "Alternative Fuels for Gas Turbine Plants - An Engineering Procurement, and Construction Contractor's Perspective," in *International Fas Turbine and Aeroengine Congress & Exhibit*, Stockholm, Sweden, 1988.

[10]   J. Nunez, *Design and development of an optically accesible high pressure combustor,* El Paso, TX, 2012.

[11]   "UCI Combustion Laboratory," University of California Irvine, [Online]. Available: http://www.ucicl.uci.edu/2/RESEARCHPROJECTS/CombustionScienceResources/TestCells/Index.aspx. [Accessed 19 July 2014].

[12]   B. Shaffer, Z. Duan and V. McDonell, "Study of Fuel Composition Effects on Flashback using a confined Jet Flame Burner," *Journal of Engineering for Gas Turbines and Power,* vol. 135, 2013.

[13]   D. Bidhan, G. Corona, M. Hayder and A. Choudhuri, "Effect of syngas composition on combustion induced cortex breadown (CIVB) flashback in a swirl stabilized combustor," *Fuel,* vol. 90, pp. 3274-3284, 2011.

[14]   S. Daniele and P. Jansohn, "Flashback propensity of syngas flame at high pressure: diagnosis and control," in *ASME turbo expo 2013: power for land, sea and air*, Glasgow, UK, 2010.

[15]   D. R. Noble, Q. Zhang, A. Shareef, J. Tootle, A. Meyers and T. Lieuwen, "Syngas Mixture Composition Effects Upon Flashback and Blowout," in *ASME Turbo Expo 2006: Power of Land, Sea and Air*, Barcelona, 2006.

[16]   S. Daniele, P. Jansohn and K. Boulouchos, "Experimental Investigatio of Lean Premixed Syngas Combustion at Gas Turbine Relevant Conditions: Lean Blowout Limits, Emmisions and Turbulent Flame Speed," in *Combustion Colloquia 2009*, 2009.

[17]   T. Lieuwen, V. McDonell, E. Petersen and D. Santavicca, "Fuel flexibility influences on premixed combustor blowout, flashback, autoignition and stability," *Journal of Engineering for*

71

Gas Turbines and Power, vol. 130, 2008.

[18] A. Gupta and D. Lilley, Swirl Flows, Cambridge, Massachusetts: Abacus press, 1985.

[19] W. York, W. Ziminsky and E. Yilmaz, "Development and Testing of a Low NOx Hydrogen Combustion System for Heavy-Duty Gas Turbines," *Journal of Engineering for Gas Turbines and Power,* vol. 135, 2013.

[20] B. Hollon, E. Steinhorsson, A. Mansour, V. McDonell and H. Lee, "Ultra-Low Emissions Hydrogen/Syngas Combustion with a 1.3 MW Injector using a Micro-Mixing Lean-Premix System," in *ASME Turbo Expo*, 2011.

[21] J. Foster and R. S. Miller, *Fundamental of High Pressure Combustion,* Clemson, South Carolina, 2010.

[22] F. S. Tool, "Premixed Flame vs Diffusion Flame- Fire Protection Engineering (FPE) Teaching Tool," firesciencetools.com, 2011.

[23] F. S. Tools, "Premixed Flame Blowoff vs Flash Back Slow Motion," firesciencetools.com, 2011.

Appendix

Appendix A - HPC Test Procedure

#	TASK	RESULT	IF ADVERSE RESULT	X or N/A
NOTE	*NOTE: BEFORE PROCEEDING WITH "TEST" ENSURE THE FOLLOWING PROCEDURES WHERE SUCCEFULY PASSED* SET-UP PROCEDURE HPC LEAK TEST PROCEDURE FLOW RATE SET-UP PROCEDURE REPEAT TEST AS NECESSARY WITHOT EXCEEDING 1 HOUR OF CONTINUOS **ACTUAL TEST** **ACTUAL TEST IS DEFINES AS THE AMOUNT OF TIME A FLAME EXIST INSIDE THE HPC CHAMBER** **FLASHBACK IS DEFINES AS THE PROPENSITY OF THE FLAME TO TRAVEL UPSTREAM**			
	Turn On video Camera (if available)	Ensure display appears in command center screen Ensure injector face is visible	N/A	
	Specify test in video Camera (If Available)	Voice recorded in camera must specify: Type of test Fuel concentration Equivalence ratio	N/A	
	Turn on Intensifier (if available) **Note: Intensifier is only to be used by qualified personnel**	N/A	N/A	
	Activate Ignition Coil	Spark must be visible	Deactivate Ignition coil Verify Signal Generator is connected Verify Battery is connected	
	Open S4 and P4	Pilot flame must be visible within 5 seconds	Close S4 and P4 Deactivate Ignition Coil Purge HPC system as specified in "flow rate set-up procedure" items	

www.manaraa.com

#	TASK	RESULT	IF ADVERSE RESULT	X or N/A
			marked with a P Verify line 4 gas tank is open and contains gas	
	Deactivate Ignition Coil	Spark must disappear inside HPC chamber	N/A	
	Open S2 and P2	Flame must be anchored in injector face	N/A	
	Open S3 and P3	Flame must be anchored in injector face	N/A	
	Open S1 and P1	Flame must be anchored in injector face	*Use emergency button in case of potential flash back*	
	If Stable: Allow flame to stabilize for 30 seconds max	Flame must be stable inside combustor	*Use emergency button in case of potential flash back*	
	Close S1 and P1	Flame must blowout	*N/A*	
	Close S2 and P2	Flame must not exist	*N/A*	
	Purge HPC system as specified in "flow rate set-up procedure" items marked with a P	P	*P*	
NOTE: REPEAT EXPERIMENTS AS NEEDED AS LONG AS THE ACTUAL TEST TIME IS NOT EXCEEDED				

Appendix B - Flow Meters Information

Range	0-5 LPM
Type	FM 1818
Serial Number	156932-1

Calibration

Voltage (v)	Flow Rate (LPM)
0.31	0.3
0.98	0.98
2.24	2.23
3.41	3.4
4.62	4.6

Range	0-30 LPM
Type	FM 1826
Serial Number	155833-6

Calibration

Voltage (v)	Flow Rate (LPM)
0.7073	4.3
1.97	12
2.726	16.5
3.298	20
4.012	24.4
4.5528	27.7

Range	0-5 LPM
Type	FM 1818
Serial Number	156932-3

Calibration

Voltage (v)	Flow Rate (LPM)
0.514	0.5
1.106	1.09
2.1155	2.11
3.227	3.23
4.2	4.2

Range	0-500 LPM
Type	FMA 1884
Serial Number	296652-2

Calibration

Voltage (v)	Flow Rate (LPM)
0.258	24
0.523	51
0.7175	70
1.04	102
1.46	145

Range	0-10 (LPM)
Type	FMA1820A
Serial Number	371766-4

Calibration

Voltage (v)	Flow Rate (LPM)
0.008	0.02
1.250	2.5
2.502	5.0
3.742	7.48
4.997	9.99

Range	0-10 LPM
Type	FMA1820A
Serial Number	371766-5

Calibration

Voltage (v)	Flow Rate (LPM)
0.008	0.02
1.253	1.253
2.499	2.499
3.750	3.750
4.998	4.998

Range	0-100 LPM
Type	FMA1842A
Serial Number	373204-2

Calibration

Voltage (v)	Flow Rate (LPM)
0	0
1.25	24.9
2.5	50.1
3.75	75
5.0	99.9

Appendix C - Calculations for Test Matrix

$$\varphi = \frac{\frac{A}{F}_{STOIC}}{\frac{A}{F}_{ACTUAL}} \quad (1)$$

$$\frac{A}{F}_{stoic\ actual} = \frac{m_{air}}{m_{fuel}} \quad (2)$$

$$\dot{m}_{fuel} + \dot{m}_{air} = \rho_{mix}\, A_o\, n\, V_o \quad (3)$$

Where:
$$V_o = V_j = S_L$$
$$A_o = Holes\ Areas$$
$$n = number\ of\ holes$$
$$V_j = S_L(1 \pm \%)$$

$$X_a = \frac{m_a}{m_{total}} \quad (4)$$

$$Y_a = \frac{moles_a}{moles_{total}} \quad (5)$$

$$\rho_{mix} = Y_{h2}\rho_{h2} + Y_{CO}\rho_{CO} + Y_{air}\rho_{air} \quad (6)$$

$$\dot{m}_{fuel} = X_{h2}\dot{m}_{fuel} + X_{CO}\dot{m}_{fuel} \quad (7)$$

INPUTS
   A.   % of H2 in fuel composition *(i.e. → .5H2+ .5CO = 50% H2 and %50 CO)*
   B. Φ

RELATIONSHIPS/DEPENDENCIES
   A.   With % of H2 and Φ we obtain→ X_{h2} , X_{h2} , X_{CO} , X_{air} , Y_{h2}, Y_{CO} , Y_{air} , ρ_{mix} and S_L

EQUATION SOLVING

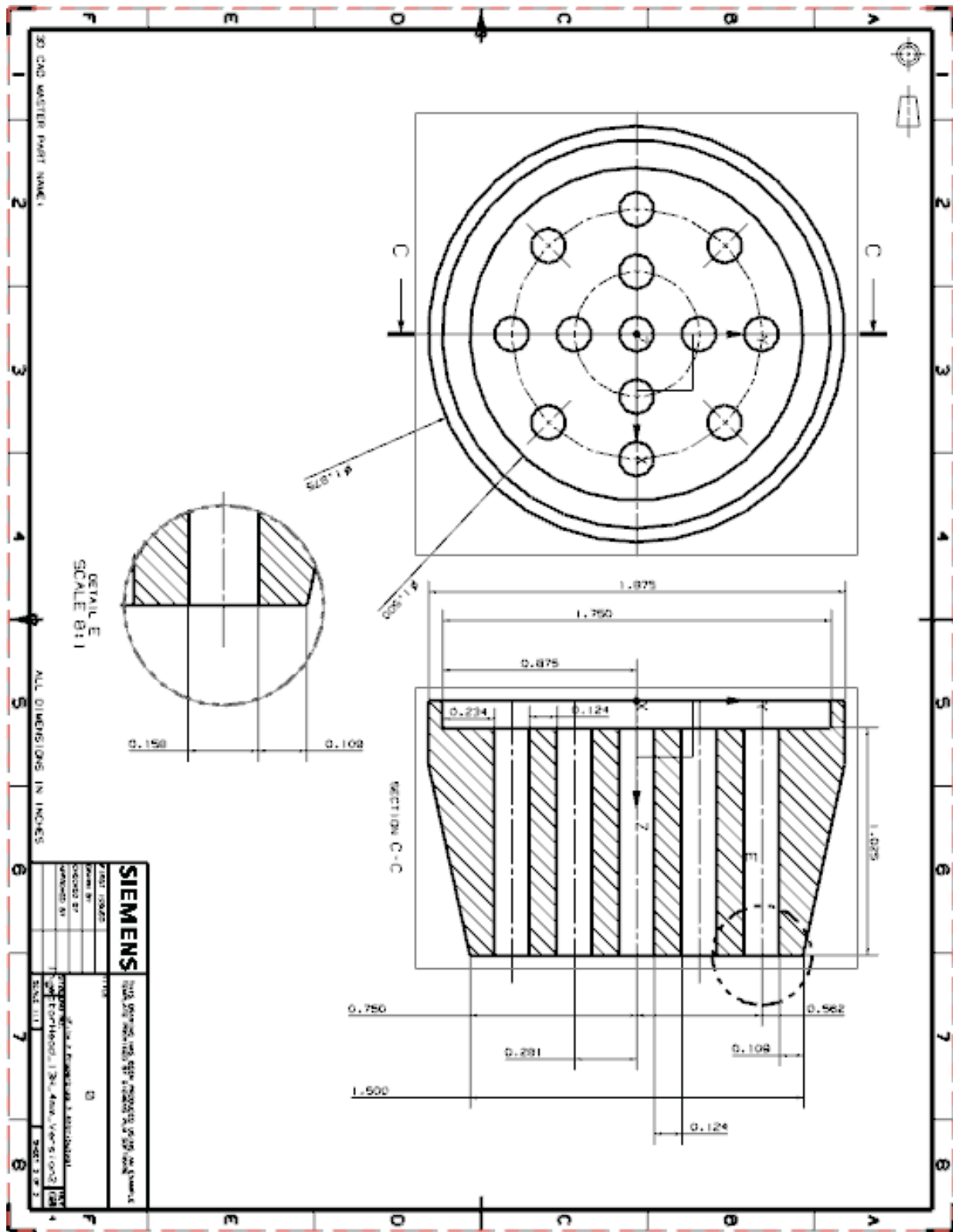$$\frac{A}{F}_{actual} = \frac{\frac{A}{F}_{stoic}}{\varphi}$$

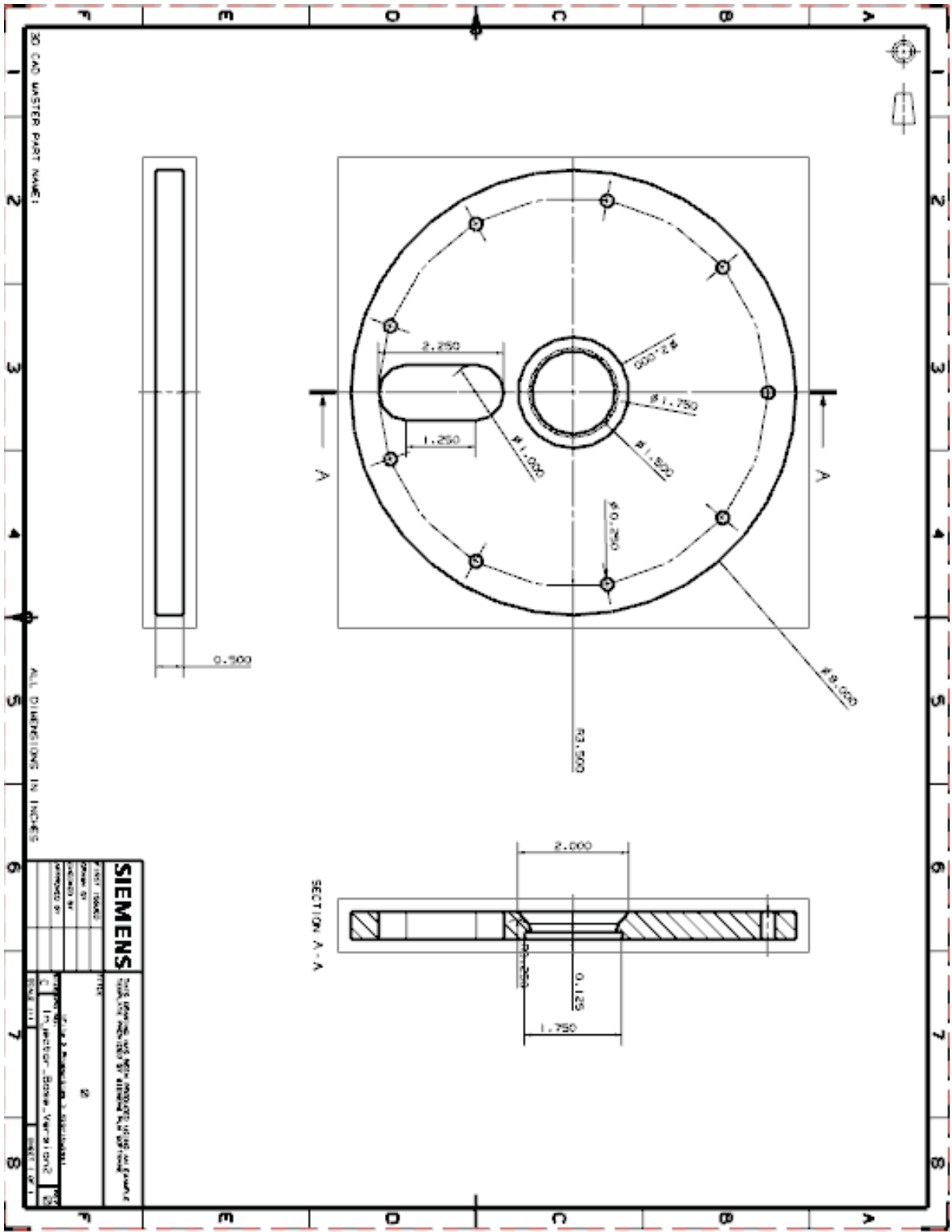$$m_{air} = \frac{A}{F}_{actual}\, \dot{m}_{fuel}$$

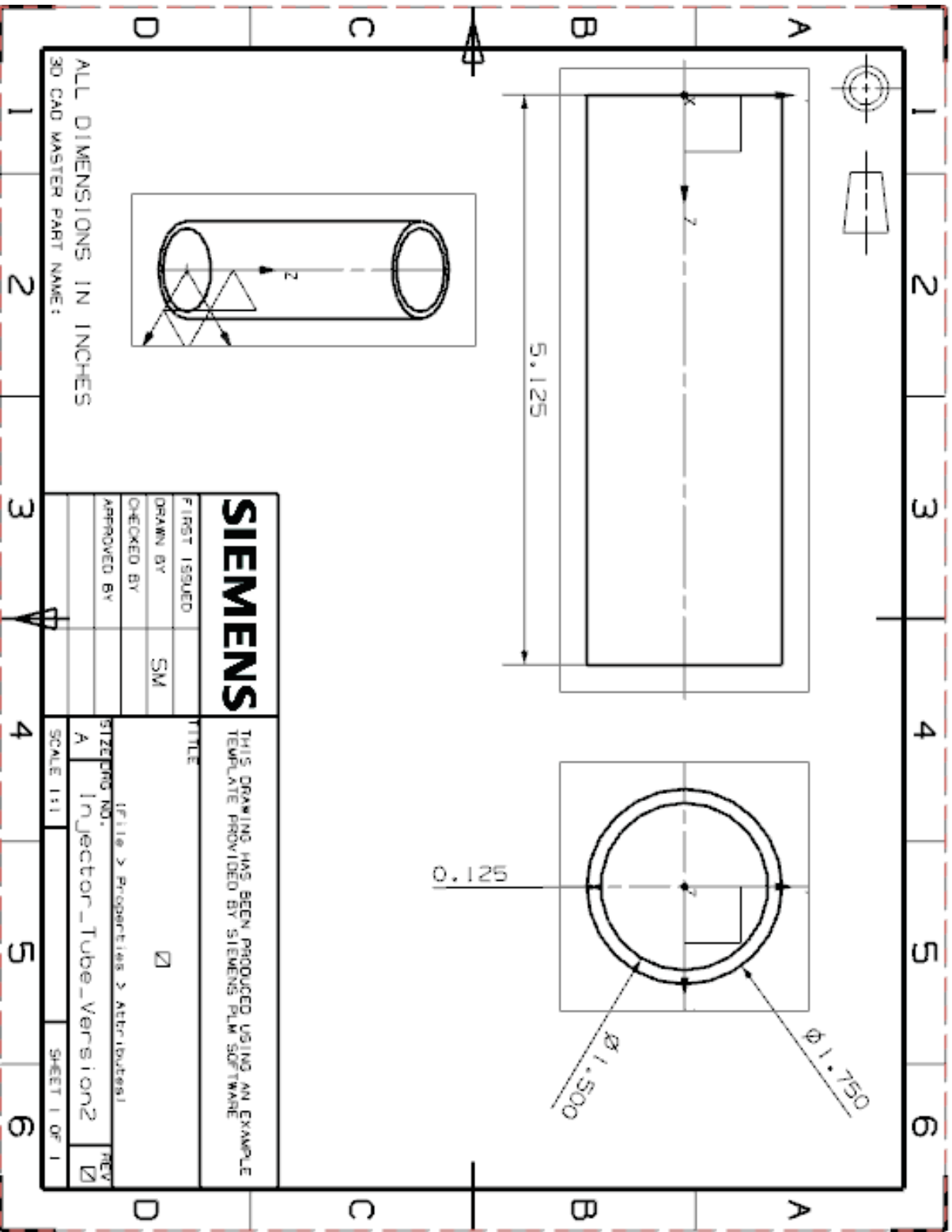$$\dot{m}_{fuel} + \frac{A}{F}_{actual}\, \dot{m}_{fuel} = \rho_{mix}\, A_o\, n\, V_o$$

$$\dot{m}_{fuel}\left(1 + \frac{A}{F}_{actual}\right) = \rho_{mix}\, A_o\, n\, V_o$$

$$\boxed{\dot{m}_{fuel} = \frac{\rho_{mix}\, A_o\, n\, V_o}{\left(1 + \frac{A}{F}_{actual}\right)}}$$

Appendix D – Multi-Tube Injector Blue Prints

SECTION A-A

SIEMENS

81

ALL DIMENSIONS IN INCHES

3D CAD MASTER PART NAME:

SIEMENS

FIRST ISSUED

DRAWN BY   SM

CHECKED BY

APPROVED BY

TITLE

(File > Properties > Attributes)

Injector_Tube_Version2

SIZE   DWG NO.   REV
A   ☑

SCALE 1:1   SHEET 1 OF 1

THIS DRAWING HAS BEEN PRODUCED USING AN EXAMPLE
TEMPLATE PROVIDED BY SIEMENS PLM SOFTWARE

5.125

0.125

Ø1.500

Ø1.750

82

www.manaraa.com

Vita

Sergio E. Maldonado is a student and a Graduate Research Assistant at the Center for Space Exploration and Technology Research (cSETR) at the University of Texas at El Paso (UTEP). Sergio moved from Jimenez, Chihuahua Mexico, where he was born and raised, to El Paso Texas in the fall of 2006 to pursue bachelors in Mechanical Engineering from UTEP. Sergio received his bachelor's degree in Mechanical Engineering in the fall of 2011. He started his graduate studies in Mechanical Engineering at UTEP working under Dr. Norman Love and Dr. Ahsan Choudhuri. While pursuing his master's degree, Sergio had the opportunity to work as a Project Engineer with United Airlines as well as to coordinate the Baja SAE UTEP 2014 competition. He has presented in various conferences such as the Southwest Energy Science and Engineering Symposium during 2013 and the UTEP Graduate School Expo in 2014. Sergio's graduate studies focus in combustion, the study of flame characteristics, and stability of syngas.

Permanent address: 213 Argonaut Dr. Apt 4

El Paso, TX, 79912

This thesis/dissertation was typed by Sergio E. Maldonado